UPPSALA
UNIVERSITET

Digital Comprehensive Summaries of Uppsala Dissertations from the Faculty of Science and Technology 315

Towards Single Molecule Imaging - Understanding Structural Transitions Using Ultrafast X-ray Sources and Computer Simulations

CARL CALEMAN

ACTA
UNIVERSITATIS
UPSALIENSIS
UPPSALA
2007

ISSN 1651-6214
ISBN 978-91-554-6911-5
urn:nbn:se:uu:diva-7915

Dissertation presented at Uppsala University to be publicly examined in D41, Biomedical Centre, Husargatan 3, Uppsala, Thursday, June 7, 2007 at 09:15 for the degree of Doctor of Philosophy. The examination will be conducted in English.

Abstract
Caleman, C. 2007. Towards Single Molecule Imaging - Understanding Structural Transitions Using Ultrafast X-ray Sources and Computer Simulations. Acta Universitatis Upsaliensis. *Digital Comprehensive Summaries of Uppsala Dissertations from the Faculty of Science and Technology* 315. 77 pp. Uppsala. ISBN 978-91-554-6911-5.

X-ray lasers bring us into a new world in photon science by delivering extraordinarily intense beams of x-rays in very short bursts that can be more than ten billion times brighter than pulses from other x-ray sources. These lasers find applications in sciences ranging from astrophysics to structural biology, and could allow us to obtain images of single macromolecules when these are injected into the x-ray beam.

A macromolecule injected into vacuum in a microdroplet will be affected by evaporation and by the dynamics of the carrier liquid before being hit by the x-ray pulse. Simulations of neutral and charged water droplets were performed to predict structural changes and changes of temperature due to evaporation. The results are discussed in the aspect of single molecule imaging.

Further studies show ionization caused by the intense x-ray radiation. These simulations reveal the development of secondary electron cascades in water. Other studies show the development of these cascades in KI and CsI where experimental data exist. The results are in agreement with observation, and show the temporal, spatial and energetic evolution of secondary electron cascades in the sample.

X-ray diffraction is sensitive to structural changes on the length scale of chemical bonds. Using a short infrared pump pulse to trigger structural changes, and a short x-ray pulse for probing it, these changes can be studied with a temporal resolution similar to the pulse lengths. Time resolved diffraction experiments were performed on a phase transition during resolidification of a non-thermally molten InSb crystal. The experiment reveals the dynamics of crystal regrowth.

Computer simulations were performed on the infrared laser-induced melting of bulk ice, giving a comprehension of the dynamics and the wavelength dependence of melting. These studies form a basis for planning experiments with x-ray lasers.

Keywords: XFEL, Ultrafast Melting, InSb, Molecular Dynamics, Water Cluster, Evaporation, Secondary Electron, Photo-cathode, Electron Scattering, Energy Loss Function, Single Particle Imaging, X-ray Diffraction, Water, Ice, KI, CsI

Carl Caleman, Department of Cell and Molecular Biology, Molecular biophysics, Box 596, Uppsala University, SE-75124 Uppsala, Sweden

ISSN 1651-6214
ISBN 978-91-554-6911-5
urn:nbn:se:uu:diva-7915 (http://urn.kb.se/resolve?urn=urn:nbn:se:uu:diva-7915)

Don't quote Jordan's lemma...

List of Pubications

Publications included in this thesis

This thesis is based on the following papers, which are referred to in the text by their numbers.

1 Tîmneanu, N., Caleman, C., Hajdu, J. and van der Spoel, D. (2004) Auger electron cascades in water and ice. *Chemical Physics*, 299:277-283

2 Harbst, M., Hansen, T. N., Caleman, C., Fullagar, W. K., Jönsson, P., Sondhauss, P., Synnergren, O. and Larsson, J. (2005) Studies of resolidification of non-thermally molten InSb using time-resolved X-ray diffraction. *Applied Physics A*, 81:893-900

3 Caleman, C. and van der Spoel, D. (2006) Temperature and structural changes of water clusters in vacuum due to evaporation. *Journal of Chemical Physics*, 125:154508

4 Caleman, C. and van der Spoel, D. (2007) Picosecond Melting of Ice by an Infrared Laser Pulse. *Submitted for publication.*

5 Ortiz, C. and Caleman, C. (2007) Secondary electron cascade dynamics in KI and CsI. *Submitted for publication.*

6 Caleman, C. and van der Spoel, D. (2007) Evaporation from water clusters containing singly charged ions. *Submitted for publication.*

Reprints were made with permission from the publishers.

Supporting publications

7 Cavalieri, A. L., Fritz, D. M., Lee, S. H., Bucksbaum, P. H., Reis, D. A., Rudati, J., Mills, D. M., Fuoss, P. H., Stephenson, G. B., Kao, C. C., Siddons, D. P., Lowney, D. P., MacPhee, A. G., Weinstein, D., Falcone, R. W., Pahl, R., Als-Nielsen, J., Blome, C., Düsterer, S., Ischebeck, R., Schlarb, H., Schulte-Schrepping, H., Tschentscher, Th., Schneider, J., Hignette, O., Sette, F., Sokolowski-Tinten, K., Chapman, H. N., Lee, R. W., Hansen, T. N., Synnergren, O., Larsson, J., Techert, S., Sheppard, J., Wark, J. S., Bergh, M., Caleman, C., Huldt, G., van der Spoel, D., Tîmneanu, N., Hajdu, J., Akre, R. A., Bong, E., Emma, P., Krejcik, P., Arthur, J., Brennan, S., Gaffney, K. J., Lindenberg, A. M., Luening, K. and Hastings, J. B. (2005) Clocking Femtosecond X Rays. *Physical Review Letters*, 94:114801

8 Lindenberg, A. M., Larsson, J., Sokolowski-Tinten K., Gaffney, K. J., Blome, C., Synnergren, O., Sheppard, J., Caleman, C., MacPhee, A. G., Weinstein, D., Lowney, D. P., Allison, T. K., Matthews, T., Falcone, R. W., Cavalieri, A. L., Fritz, D. M., Lee, S. H., Bucksbaum, P. H., Reis, D. A., Rudati, J., Fuoss, P. H., Kao, C. C., Siddons, D. P., Pahl, R., Als-Nielsen, J., Duesterer, S., Ischebeck, R., Schlarb, H., Schulte-Schrepping, H., Tschentscher, Th., Schneider, J., von der Linde, D., Hignette, O., Sette, F., Chapman H. N., Lee, R. W., Hansen, T. N., Techert S., Wark, J. S., Bergh, M., Huldt, G., van der Spoel, D., Tîmneanu, N., Hajdu, J., Akre, R. A., Bong, E., Krejcik, P., Arthur, J., Brennan, S., Luening, K. and Hastings, J. B. (2005) Atomic-Scale Visualization of Inertial Dynamics. *Science*, 308:392-395

9 Gaffney, K. J., Lindenberg, A. M., Larsson, J., Sokolowski-Tinten K., K. J., Blome, C., Synnergren, O., Sheppard, J., Caleman, C., MacPhee, A. G., Weinstein, D., Lowney, D. P., Allison, Matthews, T., Falcone, R. W., Cavalieri, A. L., Fritz, D. M., Lee, S. H., Bucksbaum, P. H., Reis, D. A., Rudati, J., Macrander, A. T., Fuoss, P. H., Kao, C. C., Siddons, D. P., Pahl, R., Moffat, K., Als-Nielsen, J., Duesterer, S., Ischebeck, R., Schlarb, H., Schulte-Schrepping, H., Schneider, J., von der Linde, D., Hignette, O., Sette, F., Chapman H. N., Lee, R. W., Hansen, T. N., Wark, J. S., Bergh, M., Huldt, G., van der Spoel, D., Tîmneanu, N., Hajdu, J., Akre, R. A., Bong, E., Krejcik, P., Arthur, J., Brennan, S., Luening, K. and

Hastings, J. B. (2005) Observation of Structural Anisotropy and the Onset of Liquidlike Motion During the Nonthermal Melting of InSb. *Physical Review Letters*, 95:125701

10 Larsson, J., Synnergren, O., Hansen, T. N., Sokolowski-Tinten, K., Werin, S., Caleman, C., Hajdu, J., Shepherd, J., Wark, J. S., Lindenberg, A. M., Gaffney, K. J. and Hastings, J. B. (2005) Opportunities and challenges using short-pulse X-ray sources. *Journal of Physics: Conference Series*, 21:87-94

11 Chapman, H. N., Barty, A., Bogan, M. J., Boutet, S., Frank, M., Hau-Riege, S. P., Marchesini, S., Woods, B. W., Bajt, S., Benner, W. H., London, R. A., Plönjes, E, Kuhlmann, M., Treusch, R., Düsterer, S., Tschentscher, Th., Schneider, J. R., Spiller, E., Möller, T., Bostedt, C., Hoener, M., Shapiro, D. A., Hodgson, K. O., van der Spoel, D., Burmeister, F., Bergh, M., Caleman, C., Huldt, G., Seibert, M. M., Maia, F. R. N. C., Lee, R. W., Szőke, A., Tîmneanu, N. and Hajdu, J. (2006) Femtosecond diffractive imaging with a soft-X-ray free-electron laser. *Nature Physics*, 2:839-843

12 Hau-Riege, S. P., Chapman, H. N., Krzywinski, J., Sobierajski, R., Bajt, S., London, R. A., Bergh, M., Caleman, C., Nietubyc, R., Juha, L., Kuba, J., Spiller, E., Baker, S., Bionta, R., Sokolowski-Tinten, K., Stojanvic, N., Kjornrattanawanich, B., Gullikson, E., Plönjes, E., Toleikis, S. and Tschentscher, Th. (2007) Subnanometer-scale Measurements of the Interaction of Ultrafast Soft X-ray Free-Electron-Laser Pulses with Matter. *Physical Review Letters*, 98:145502

13 Hau-Riege, S. P., London, R. A., Bionta, R. M, McKernan, M. A., Baker, S. L., Krzywinski, J., Sobierajski, R., Nietubyc, R., Pelka, J. B., Jurek, M., Juha, L., Chalupský, J., Cihelka, J., Hájková, V., Velyhan, A., Krása, J., Kuba, J., Tiedtke, K., Toleikis, S., Tschentscher, Th., Wabnitz, H., Bergh, M., Caleman, C., Sokolowski-Tinten, K., Stojanic, N. and Zastrau, U. (2007) Damage threshold of inorganic solids under free-electron-laser irradiation at 32.5 nm wavelength. *Applied Physics Letters*, 90:173128

14 Chalupský, J., Juha, L., Kuba, J., Cihelka, J., Hájková, V., Koptyaev, S., Krása, J., Velyhan, A., Kuba, J., Bergh, M., Caleman, C., Hajdu, J., Bionta, R. M., Chapman, H., Hau-Riege, S., London, R. A., Jurek, M., Krzywinsk, J., Nietubyc, R., Pelka, J. B., Sobierajski, R., Meyer-ter-Vehn, J., Krenz-Tronnier, A., Sokolowski-Tinten, K., Stojanovic, N., Tiedtke, K., Toleikis, S., Tschentscher, T., Wabnitz, H. and Zastrau, U. (2007)

Characteristics of focused soft X-ray freeelectron laser beam determined by ablation of organic molecular solids. *Optics Express*, 15:6036-6043

15 Chapman, H. N., Hau-Riege, S. P., Bogan, M. J., Bajt, S., Barty, A., Boutet, S., Marchesini, S., Frank, M., Woods, B. W., Benner, W. H., London, R. A., Rohner, U., Szőke, A., Spiller, E. A., Möller, T., Bostedt, C., Shapiro, D. A., Kuhlmann, K., Treusch, R., Burmeister, F., Bergh, M., Caleman, C., Huldt, G., Seibert, M. M., and Hajdu, J. (2007) Femtosecond Time-Delay X-ray Holography. *Submitted for publication*

16 Chalupský, J., Juha, L., Kuba, J., Cihelka, J., Hájková, V., Bergh, M., Bionta, R. M., Caleman, C., Chapman, H., Hajdu, J., Hau-Riege, S., Jurek, M., Koptyaev, S., Krása, J., Krenz-Tronnier, A., Krzywinsk, J., London, R., Meyer-ter-Vehn, J., Nietubyc, R., Pelka, J. B., Sobierajski, R., Sokolowski-Tinten, K., Stojanovic, N., Tiedtke, K., Toleikis, S., Tschentscher, T., Velyhan, A., Wabnitz, H. and Zastrau, U. (2007) Ablation of organic molecular solids by focused soft X-ray free-electron laser radiation, *X-Ray Lasers 2006 Proceedings of the 10th International Conference, Springer Proceedings in Physics, vol 115, Eds. Nickles, P.V. and Janulewicz, K.A. Springer-Verlag, Berlin-Heidelberg-New York, pp. 503-510*

Contents

Abbreviations

EOS	Electro Optic Sampling
ESI	Electrospray Ionization
FEL	Free Electron Laser
FLASH	Free Electron Laser in Hamburg
fs	femtosecond
GROMACS	Groningen Machine for Chemical Simulations
IR	Infra Red
LCLS	Linac Coherent Light Source
LJ	Lennard-Jones
MD	Molecular Dynamics
MS	Mass Spectroscopy
PBC	Periodic Boundary Conditions
PME	Particle-mesh Ewald
PPPM	Particle-Particle Particle-Mesh
QM	Quantum Mechanic
SASE	Self Amplified Spontaneous Emission
SCSS	Spring-8 Compact Sase Source
SLAC	Stanford Linear Accelerator Center
SPC	Single Point Charge
SPPS	Sub Pico-second Pulse Source
TPP	Tanuma, Powell and Penn
TTF	Tesla Test Facility
VUV	Vacuum Ultra Violet
XFEL	X-ray Free Electron Laser

1. Introduction

Much of what we know about the detailed structure of biomolecules, including proteins, DNA and RNA, has come through the use of x-ray diffraction. Synchrotron radiation has revolutionized this field, enabling studies of larger and more complex systems at increasingly high levels of resolution on smaller (often micron-sized) samples. The key to this success has been the use of Bragg diffraction from multiple copies of oriented molecules in a single crystal. However, there are classes of proteins (as well as many other types of materials) that are difficult or impossible to crystallize, including membrane proteins and many glycoproteins, for which a high resolution means of structure determination would be invaluable (Neutze et al., 2000, 2004).

On current synchrotron-based x-ray microscopes, where optics have steadily been improving, the highest resolution that can be achieved on living systems has reached a limit imposed by radiation damage. This resolution limit is about 20 nm or less, and is caused mainly by chemical changes, diffusion, and local heating over time scales greater than microseconds. This barrier to resolution can be removed (or substantially reduced) by using intense x-ray pulses, of duration shorter than any process that causes structural changes over the resolution length of interest. This concept of flash imaging can be extended all the way to atomic resolution where it seems possible that single molecules could be imaged (Neutze et al., 2000). The experimental method of choice to perform high resolution imaging, from resolutions of 20 nm to below 0.2 nm, is single particle diffraction. Figure 1.1 shows a schematic picture of the planned single molecule experiments.

Early analyses of the dynamics of damage formation (Solem, 1986; Hajdu, 1990) suggested that the damage barrier (Henderson, 1995) of about 200, 12 keV photons per $Å^2$ could be extended using a very intense x-ray beam and very short exposures. This led to the prediction that atomic structures could be retrieved from single molecule samples, omitting the crystallization (Neutze et al., 2000; Hajdu et al., 2000; Hajdu, 2000).

Bombarding molecules with x-rays ionizes the atoms, and the molecule will break up due to repulsive Coulomb forces between the ions. In a crystalline sample the ionization is spread out among a large number of individual molecules, which reduces the damage effect on the diffraction pattern.

In a single molecule sample this is not the case. To image a non-crystalline sample, the photon pulse therefore must be shorter than the time it takes the molecule to explode, and the pulse has to be intense enough to generate a interpretable diffraction pattern from a single pulse.

The question is how short and intense a pulse has to be to achieve that. This problem has been addressed in a number of theoretical publication, by simulating the photon material interaction and the dynamics of highly ionized, biologically relevant samples (Neutze et al., 2000; Bergh et al., 2004; Hau-Riege et al., 2004; Jurek et al., 2004b,a). The conclusion from these calculations seems to be that pulse lengths shorter than 100 fs and intensities higher than 10^{11} photons per pulse are needed, focused to a 100 nm spot.

A more recent estimation of the maximum admissible pulse length, including image classification and structure reconstruction from diffraction data (Huldt et al., 2003), was published by Hau-Riege et al. (2005), who concluded that an x-ray pulse shorter than ten femtoseconds is needed to get atomic resolution images of biological samples with 12 keV photons.

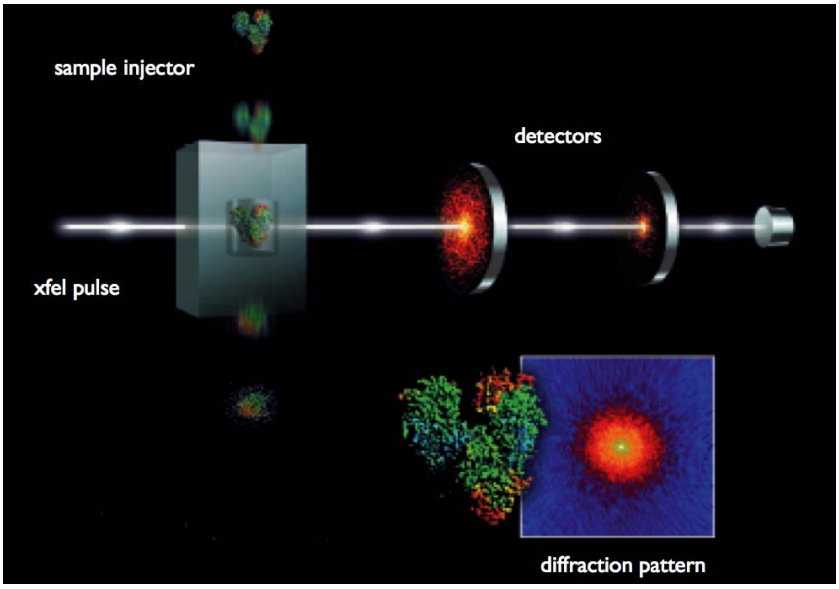

Figure 1.1: Scheme of the planned single molecule imaging experiment (www-ssrl.slac.stanford.edu/lcls/). A large number of challenges have to be overcome to solve the first structure using this technique.

Techniques for image alignment and averaging have been developed for cryoelectronmicroscopy (Frank, 1996; van Heel et al., 2000), and these methods could be adopted for aligning and averaging diffraction images. A 3D diffraction reconstruction would then lead to the atomic-level

structure of the molecule. However, the challenges in carrying out such an experiment are formidable. Among the challenges is the need for "containerless packaging" so that only the sample will be imaged and the development of advanced reconstruction algorithms (Huldt et al., 2003) for averaging and inverting the diffraction images into the real space molecule. In principle, there is a direct way to determine the phases required for the inversion using an approach called "oversampling" (Sayre, 2002) but again much remains to be done to make this approach practical in real circumstancess (Miao et al., 2001, 2006, 2003; Robinson et al., 2001; Marchesini et al., 2003a,b).

1.1 Diffraction imaging

The diffraction pattern of an object is proportional to the squared modulus of the molecular transform (the three-dimensional Fourier transform of the electron density). The coordinates of the diffraction space, usually called reciprocal space, are those of the scattering vector (or momentum transfer vector) between the incident and scattered x-rays.

Conventional macromolecular crystallography requires high quality single crystals, and in an x-ray diffraction experiment, crystals are exposed to a parallel beam of x-rays with a planar wave front to obtain a three-dimensional diffraction data set. This is done by rotating the crystal in the beam, and bringing all possible lattice planes into diffracting position, where the Bragg condition is satisfied. Data points from such an experiment provide a discrete sampling of the Fourier transform of the object at points where the crystal lattice permits us to observe this transform through the Bragg peaks (Figure 1.2).

In order to reconstruct the electron density, reciprocal space must be sampled with sufficient density (Shannon, 1949) and the diffracted intensities must be known with an acceptable accuracy. Bragg diffraction peaks of a crystal provide a critical sampling of the Fourier transform (Sayre, 1952), and hence the phase problem of crystallography.

When a coherent diffraction pattern is sampled at spacings sufficiently finer than the Bragg peak frequency (i.e. the inverse of the sample size), the phase information is in principle encoded inside the diffraction intensities (Bernal et al., 1938; Bragg and Perutz, 1952), and can be directly retrieved by using an iterative process (Gerchberg and Saxton, 1972). In combination of this oversampling phasing method with either coherent x-rays or electrons, a novel form of diffraction microscopy has recently been developed to image nanoscale materials and biological structures.

Today, there are over 40,000 entries in the Protein Data Bank (http://www.pdb.org), 85% of which are x-ray crystal structures. This

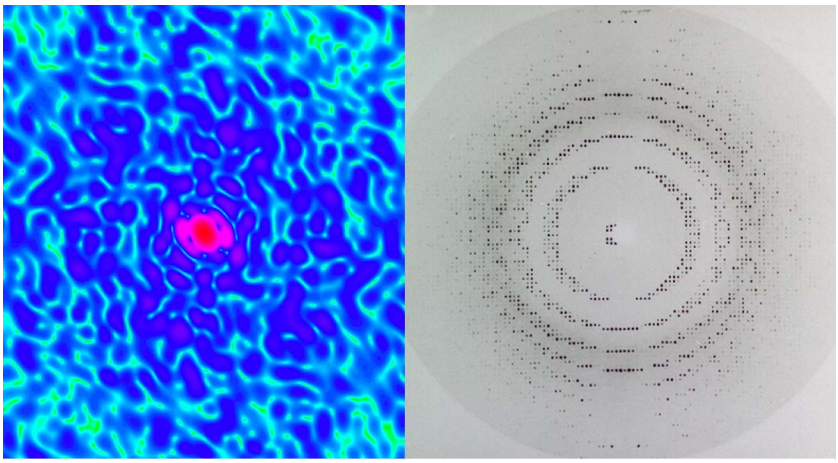

Figure 1.2: Diffraction pattern from a lysosyme, single molecule (left) and from a crystal of (right). In the discrete pattern the continuous diffraction image is seen only where the Bragg peaks allow it. The continuous data set is simulated from a lysozyme (Neutze et al., 2000), and the discrete pattern was collected by J. Hajdu at the Daresbury Synchrotron Radiation Source.

number is somewhat inflated by the large number of related structures, such as structures from homologous proteins from different sources etc, but it is still a large number, considering that the human body contains less than 100,000 different proteins (Dobson, 2004). Most of the structures in the Protein Data Bank were solved by conventional crystallographic phasing techniques, but in a handful of cases it was possible to exploit oversampling via solvent flattening and averaging methods, including averaging between different crystal forms of the same molecule, or using non-crystallographic symmetry.

To be able to solve the structure of non-crystallizable proteins is of course of great interest, but maybe even more important would be to solve the atomic structures of larger biological object such as a cell. The ability to extract the atomic structures from any nanoscale-micrometer object will be a large step in structural science and the potential impact on medicine can not be overestimated.

X-ray sources capable of generating pulses with a pulse length in the femtosecond regime and with a peak brilliance 10 orders of magnitude higher than conventional third generation synchrotron are available today. The first operational soft x-ray free electron laser (XFEL) in the world is the FLASH facility in Hamburg (Free electron LASer in Hamburg at the Deutsches Elektronen-Synchrotron DESY, http://vuv-fel.desy.de/). A second source, also in the soft x-ray regime, is the Spring-8 Compact

Sase Source (SCSS) (http://www-xfel.spring8.or.jp/) in Japan. In the near future the Linac Coherent Light Source (LCLS) (http://www-ssrl.slac.stanford.edu/lcls/) at the Stanford Linear Accelerator Center will be operational as the first hard x-ray FEL with wavelengths down to 1.0 Å). The interest in FELs is large and a considerable number of new FEL facilities are being planned around the world; the FERMI facility in Trieste, the BESSY-FEL in Berlin, SPARC in Rome, and DUVFEL in Brookhaven.

There are many interesting problems left that will have to be solved before the first atomic structures can be determined using this technique.

1.2 Scope of the thesis

The work presented in this thesis addresses some of the problems facing peak brightness experiments at FEL sources. These experiments exploit the extreme brightness and the high peak brilliance of a focused FEL pulse. The list of challenges can of course be made very long, but nevertheless the hope is that this thesis will add some pieces to the puzzle. The work is relevant to a broad range of fields where high resolution structural and temporal information is valued.

Understanding of photon-material interaction is fundamental in many aspects of structural studies. Not only to answer the question whether one can rapidly image an exploding sample before the effects of the x-ray damage destroy all useful structural information, but also in aspects such as pump-probe synchronization and the use of x-ray optics. A majority of the papers in the list of publications deals with such topics.

The experiments will be done in vacuum to assure that the data recorded from a single shot image is as noise free as possible. Therefore understanding of the behavior of molecules under such conditions is essential for single particle imaging.

This thesis is structured as follows. The first part presents the tools, the x-ray sources used in this work (Chapter 2) and the basis of the molecular dynamics calculations used here (Chapter 3).

Chapter 4 presents sample handling. Papers 3 and 6 are put into the context of single molecule imaging, and the results are related to the knowledge about the behavior of biomolecules in vacuum.

Chapter 5 treats high energy photon interaction and is directly related to Papers 1 and 5. It gives the background to the studies and discusses the relevance of the results to damage calculations.

Chapter 6 describes time resolved x-ray studies, and the importance of the timing between the pump pulse (for example from an optical laser) and the probe pulse (from the x-ray source). The chapter treats experiments presented in Papers 2 and 7-10. Paper 5 presents calculations of the ex-

pected time resolution of two substances used for making photocathodes, and is also related to time resolved studies using pump-probe techniques.

Chapter 7 introduces phase transitions, and presents Papers 2 and 4. Both papers treat laser induced structural changes in crystals, one is an experimental study and the other is based on computer simulations.

The final chapter gives an outlook.

2. X-ray sources

This chapter gives a short overview of three x-ray sources relevant for this work. A number of different x-ray sources are utilized for structural studies. These sources differ in many ways, such as photon energy and intensity, and therefore, they are appropriate for different types of research. In general the pulse length limits the time resolution, the photon energy limits the length resolution, and the photon intensity and the timing accuracy limits the signal to noise ratio. All these factors are important for the studies presented here.

Table 2.1: Performance of x-ray sources used in this work. The data presented are taken from Papers 2, 8 and 11, and from references (Ayvazyan et al., 2006; Synnergren, 2005; Düsterer et al., 2006). † estimated numbers, * after the monochromator (the repetition rate of MAX II is 100 MHz)

Machine	Photons/pulse	Pulse length	Photon energy	
		(FWHM)	eV	Å
MAX II (D611)	5×10^3*	100 ps	3-8×10^3	1.55-4.00
SPPS	2×10^6	80 fs	9×10^3	1.4
FLASH	10^{13}	10-30 fs	12-200	62-103
LCLS†	3×10^{12}	100 fs	8×10^3	1.55

2.1 MAX II, Lund, Sweden

MAX-lab is a National Synchrotron Radiation Facility in Lund, and it houses a linear accelerator (LINAC) injector and three electron-storage rings. In the work described here, the 1.5 GeV MAX II ring was used (Figure 2.1). MAX II is a third generation electron storage ring, producing synchrotron radiation in the x-ray domain. Experiments presented in Paper 2 were performed at beam line D611. In a synchrotron, electrons circulate in the storage ring, emitting radiation as their trajectories bend. This way they lose energy and

to compensate for this, a radio frequency accelerating cavity gives the electrons a small momentum impulse to replenish lost energy each time they pass. The radiator used at beam line D611 is a dipole bending magnet. At synchrotrons undulators and wigglers are also commonly used radiators. The magnets of bending magnets, undulators or wigglers force the electron beam on curved trajectories, and the change of velocity generates electron magnetic radiation.

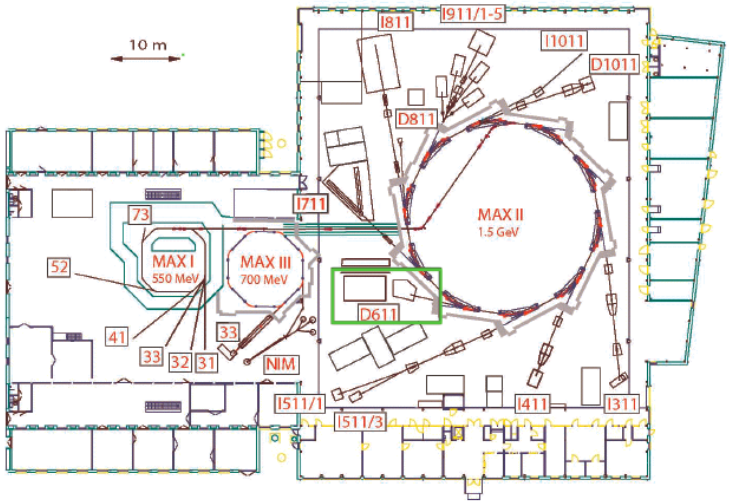

Figure 2.1: Layout of MAX-lab with its three storage rings. Beamline D611 at MAX II was used in this thesis. MAX II is 1.5 GeV third generation electron storage ring for producing synchrotron radiation. The figure is adopted from www.maxlab.lu.se.

Synchrotrons are excellent light sources for producing a stable and intense x-ray beam with a large number of photons per second and very low divergence. Over the past 30 years, synchrotron radiation became standard in many research areas, and are routinely used for the determination of protein structures from crystalline samples, for solution and gas phase scattering experiments on a variety of substances, and for a range of spectroscopic studies. Synchrotrons have long pulses with duration in the range of 10-400 ps. This makes synchrotron sources suitable for studies on dynamic phenomena with nanosecond time resolution, as in Paper 2. However, synchrotrons are not particularly useful to study dynamics on a sub picosecond time scale (or for single particle imaging), since sample will be destroyed way before enough photons have reached the detector.

2.2 SPPS, Standford, California, USA

The Sub Picosecond Pulse Source (SPPS), at the Stanford Linear Accelerator Center (SLAC) in California, was the first accelerator-based femtosecond x-ray source, operating in the hard x-ray domain. SPPS connects femtosecond spectroscopy with femtosecond structural methods. It was active between 2003 and 2006 and produced pulses of spontaneous x-ray radiation utilizing the electron beams from the LINAC at SLAC (Figure 2.2). The electrons

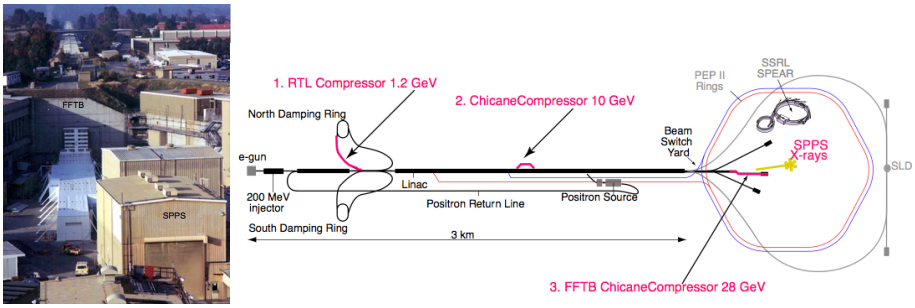

Figure 2.2: Layout of the Sub-Picosecond Pulse Source (SPPS). SPPS is an accelerator-based hard x-ray source to produce femtosecond x-ray pulses. It uses the full length of the SLAC linac and injects 28 GeV electron bunches into an undulator magnet. SPPS is not a FEL, it produces spontaneous radiation from the undulator. FFTB: Final Focus Test Beam. (Image, courtesy SLAC.)

were injected into an undulator with a fundamental energy of 9 keV (1.4 Å) at 28.5 GeV electron energy (Emma, 2002; Bentson et al., 2002; Akre et al., 2002). Two sets of multilayer mirrors directed the beam to the experimental hutch, reducing the energy bandwidth ($\Delta E/E$) to about 1%. One of these mirrors was resonant for the fundamental energy, and the other for the third harmonic. SPPS had all components of a free-electron laser but the undulator was too short bo be suitable for lasing. As a consequence, the number of photons per pulse at SPPS was not sufficiently high for single molecule imaging, but SPPS was eminently suitable for studying ultrafast structural transitions, including phase transition processes (resulting in Papers 8, 9, 10 and Fritz et al. (2007)). SPPS was also an important ground for testing and developing some of the principles of the XFEL.

2.3 FLASH, Hamburg, Germany

FLASH (Figure 2.3) is the first free electron laser (FEL) to reach the soft x-ray domain. It operates on the principle of self amplified spontaneous emission (SASE). An electron bunch accelerated in a LINAC passes through an un-

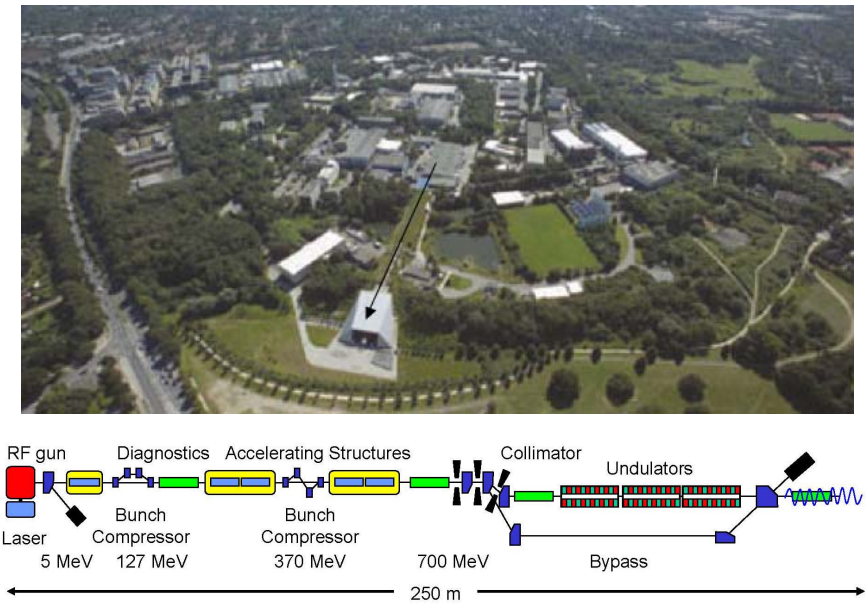

Figure 2.3: Outline of the FLASH soft x-ray laser at DESY, Hamburg. FLASH is the first free-electron laser to produce ultrashort photon pulses with wavelength reaching the x-ray domain.

dulator, consisting of a series of magnets with alternating field direction. In the undulator the electron bunch starts radiating due to acceleration produced by periodically changing the velocity of electrons as the electrons swing in and out horizontally when passing along the undulator magnet. At wavelengths longer than or comparable to the bunch length, the radiation generated from the electron bunch is coherent.

The electromagnetic field from the radiating electrons modulates the structure of the electron bunch, such that the electrons that are located before the phase of the field lose energy while the electrons located after the phase gain energy. This leads to a micro bunching within the electron bunch. Since the radiating micro bunches of electrons are spaced with the distance one wavelength of the light they radiate, whey will all radiate in phase. In other words, they are lasing, hence the name “free electron laser”. The coherent radiation intensity is proportional to the square of the number of electrons in the bunch. The amplification of the emitted radiation takes place in three stages, illustrated by Figure 2.4. In the beginning of the undulators (I) the microbunches start to form. The wave grows roughly as the cube of the distance. In region II the gain is exponential and in the third region (III) the amplification saturates and the

energy will oscillate between the electron and the photon beam. This is because the electrons will stop gaining energy from the wave.

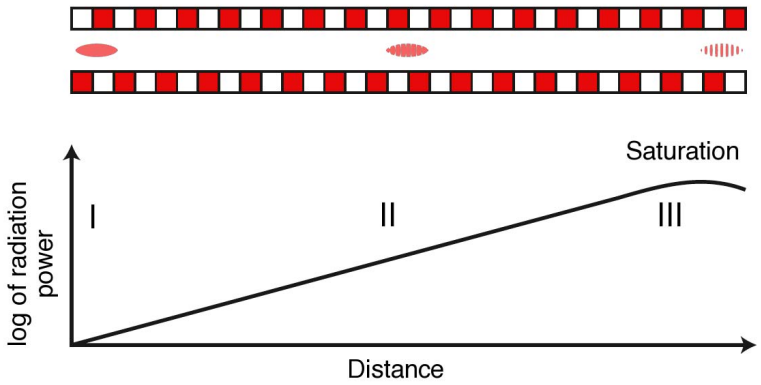

Figure 2.4: Evolution of the Self Amplified Spontaneous Emission effect along the undulator.

The SASE FEL principle at short wavelengths was first demonstrated to work at the Tesla Test Facility (TTF) in Hamburg (Andruszkow et al., 2000; Ayvazyan et al., 2002b,a), at a wavelength of 100 nm. TTF was a pilot facility mainly used for machine development. Later TTF was closed and rebuilt as TTF-2, which later got the catchy name of Free Electron Laser in Hamburg (FLASH). FLASH is, in contrast to TTF, a user facility where research communities from many different fields can take advantage of the intense beam. Originally operating at a wavelength of 32 nm, FLASH has continuously been modified to work at shorter and shorter wavelengths. As this is written the wavelength is down to around 13 nm, and the machine will reach 6 nm by autumn 2007. These wavelengths are not yet suitable for atomic resolution structural studies, but they are suitable of imaging larger objects with nanometer resolutions. There are still a lot of steps toward single particle imaging that have and will be taken at FLASH. Recent publications based on experiments executed at FLASH, have provided knowledge about damage by FEL pulses in the soft x-ray regime (Papers 12-14 and 16). The principle of reconstruction of an image of a sample that is completely destroyed during the x-ray exposure was also proven at FLASH, illustrated by Figure 9.1 (Paper 11).

3. Molecular Dynamics

The main theoretical tool used in this thesis is Molecular Dynamics (MD), implemented in the GROMACS software package (Berendsen et al., 1995; Lindahl et al., 2001; van der Spoel et al., 2005). MD is a powerful instrument for describing the dynamics of molecular systems. MD is based on simple principles, but it can be used to describe nature quite accurately on a mesoscopic scale if handled with care (Allen and Tildesley, 1987). In MD atoms, ions and sometimes small groups of atoms are considered as soft spheres whose interactions are described using force fields calculated from potentials. At every time step in a simulation the pairwise forces between all interaction points (be it an atom, an ion or a group of such) are calculated. When this is done for the complete system Newton's equation of motion (Newton, 1687) are integrated and all interaction points are moved to new positions. The procedure is then performed with the atoms at the new positions, and so forth. By keeping the time step short enough, such that each atom only moves a very short distance (compared to the distance between two atoms in the system), no unrealistic forces will occur and the algorithm is stable.

Newton's equation of motion:

$$m_i \frac{\partial^2 r_i}{\partial t^2} = F_i, \qquad i = 1,2,....N, \tag{3.0.1}$$

is solved at every time step for each of the N interaction points i, r_i is the position of interaction point i and m_i its mass, and t time and, where the forces F_i are the negative derivative of the potential $V(r_1, r_2, ...r_N)$

$$F_i = -\frac{\partial V}{\partial r_i}. \tag{3.0.2}$$

The potential V is described by the Coulomb potential (treating interactions due to charged particles)

$$V_{\mathrm{r}}^{\mathrm{c}} = \frac{1}{4\pi\varepsilon_0}\left(\frac{q_i q_j}{r_{ij}}\right), \tag{3.0.3}$$

(where r_{ij} is the distance between the two charges q_i and q_j) and the Lennard-Jones (LJ) potential, which is repulsive at short distances (as a result of overlapping electron orbitals, due to Pauli repulsion (Massimi,

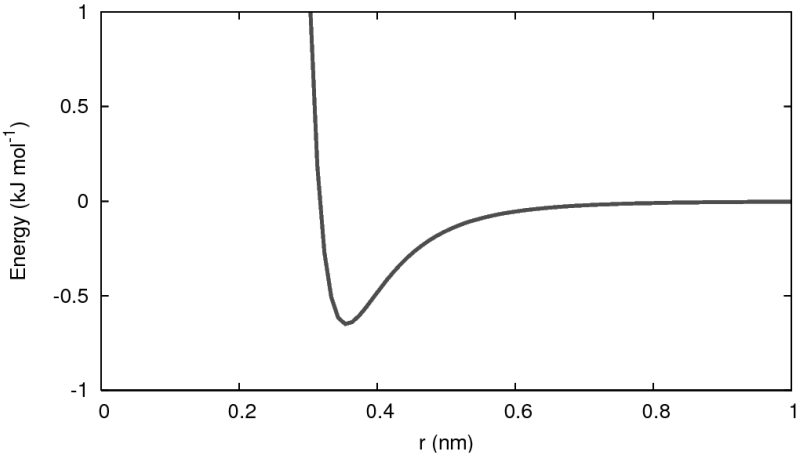

Figure 3.1: Lennard-Jones potential for single point charge (SPC) water (Berendsen et al., 1981).

2005)) and attractive at long distances, due to the Van der Waals forces

$$V_{\mathrm{r}}^{\mathrm{lj}} = 4\varepsilon \left[\left(\frac{\sigma}{r_{ij}} \right)^{12} - \left(\frac{\sigma}{r_{ij}} \right)^{6} \right] \tag{3.0.4}$$

The LJ potential is based on parameters, σ and ε that are fitted to reproduce experimental data or deduced from quantum chemical calculations. Figure 3.1 shows the LJ potential for a common water model.

As for any tool, it is important to be aware of the limitations of MD. Using MD without critically reviewing input and comparing results with experiments whenever possible, will produce results that stand on a fragile foundation. The main approximations of MD (as implemented in GROMACS) are listed below.

The simulations are classical. Classical mechanics is used to describe the motions of atoms, leaving out any quantum effects, such as tunneling through energy barriers. This approximation is acceptable for most atoms as long as the temperature does not reach extreme values. For describing light atoms, like hydrogen and helium, quantum mechanics (QM) play a more expressed role. When the resonance frequency in bonds or bond angle vibration approaches $k_{\mathrm{B}}T/h$, these are not correctly simulated, due to the classical treatment.

Electrons are in the ground state. The motion of electrons are not considered in classical MD, the electrons are assumed to adjust their dynamics instantly compared to the positions of the atoms, an approach known as the Born-Oppenheimer approximation. This is acceptable as long as the system

is not perturbed, e.g. ionized or otherwise electronically excited. The limit for laser-matter interactions is discussed in Paper 4, where infrared (IR) laser radiation is absorbed in ice through stimulating bond vibrations. To describe x-ray induced ionization effects using MD simulations, as is done in references (Bergh et al., 2004; Neutze et al., 2000; Jurek et al., 2004b), a treatment of electron trajectories and free electron ejection as well as cross sections for photon and electron interaction must be included. One way to do so is by treating the electrons as an electron gas (Bergh et al., 2004).

Force fields are approximate. Forces in MD are described by force fields. These force fields are adapted to fit experimental data as well as possible, but there will always be some discrepancy between the experimental data and the fit.

The force field is pair-additive. Force interactions are calculated pair wise and then added together, which means that any multi-body effects are assumed to be the sum of multiple pair interaction.

Long-range interactions are cut-off. GROMACS normally uses a cut-off for the LJ interactions and Coulomb interactions. The cut-off range can not exceed the half of the simulation box side for a system with periodic boundary conditions (PBC), since the same particle should only be accounted for once. For large neutral systems this is not a problem, but for polarizable systems or systems containing charges this is expected to become a problem. In such cases long-range electrostatic algorithms, such as Ewald summation (Ewald, 1921), the Particle-mesh Ewald (PME) method (Darden et al., 1993) or the Particle-Particle Particle-Mesh (PPPM) method (Hockney and Eastwood, 1981) can be used. Using PBC the dipole from polarizable molecule models in an external electric field might induce an effective electric field that is not realistic. In Paper 4 such effects are discussed. In the cluster evaporation simulations (Papers 3 and 6) no cut-offs are used at all.

Boundary conditions are unnatural. Since only a finite number of particles can be simulated the system will be spatially defined by unnatural boundaries. Either a cluster of molecules can be put in vacuum, which might be an undesirable feature, or when simulating material in bulk, PBC can be used. PBC may induce an artificial order to the system (van der Spoel and van Maaren, 2006) , but for a large system the errors are small. In some cases though, as in Papers 3 and 6, the vacuum environment might actually be desirable.

3.1 Molecular models

In MD molecules are constructed by putting rigid or flexible bonds between atoms. Bond lengths and angles are usually taken from crystallographic data and force constants from spectroscopy. The

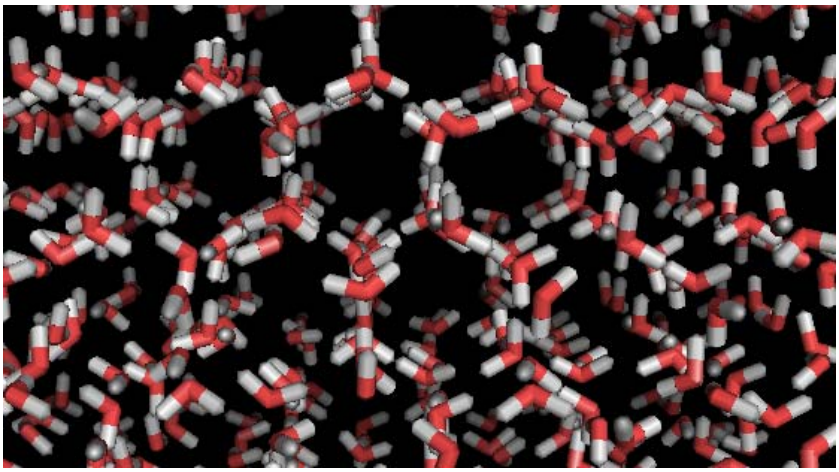

Figure 3.2: The structure of hexagonal ice, the most common type of ice in nature. The structure is taken form reference (Hayward et al., 1997).

charges are fitted to QM electrostatic potentials or treated as empirical parameters (Allen and Tildesley, 1987). LJ parameters and charges are tuned such that simulations reproduce experimental data. A specific molecule model is constructed such that it reproduces a limited set of physical parameters. It is therefore crucial to consider what physical parameters a molecular model is tuned to, before any conclusions about the results of a simulation are drawn (Leach, 2001).

Water is the main molecule simulated in Papers 1, 3, 4 and 6. Even for a molecule of such simple structure as water none of the over 50 water models presented in the literature can reproduce all the physical properties of water (Guillot, 2002). In Paper 3, this fact is discussed and three different commonly used water models are compared; SPC (Berendsen et al., 1981), TIP4P (Jorgensen et al., 1983) and TIP5P (Mahoney and Jorgensen, 2000). The simulations in Paper 4 include absorption of an external electric field, it was therefore necessary to employ a flexible water model developed to do so (Lawrence and Skinner, 2003).

Very recently, a force field was presented for water, developed entirely from first order calculations (Bukowski et al., 2007). This forcefield predicted successfully the properties of a water dimer, as well as of liquid water, in good agreement with experiments. This raises hope for models, which could be particularly use full for detailed studies of laser-matter interaction.

4. Handling hydrated samples

With ultrasmall samples, standard procedures for sample selection, characterization and handling can not be applied. Everything within the beam-path will interact with x-rays, and contribute to the image, including gas molecules and the sample holder. It is therefore necessary to develop container-free new methods, and inject samples directly into a vacuum chamber to assure a continuous flow of molecules into the interaction zone with the x-ray pulse (Hajdu et al., 2000; Neutze et al., 2000, 2004). Figure 1.1 shows the suggested experimental arrangement.

Sample injection can be done by spraying techniques. One such technique is electrospray ionization (ESI). ESI was developed in the 1960s to inject biomolecules into the gas phase for mass spectrometry (MS) (Dole et al., 1968; Yamashita and Fenn, 1984a,b), and it was awarded with the Nobel Prize in Chemistry in 2002. Biomolecules sprayed into vacuum will be in random orientation, encapsulated in a micro-droplet (Kebarle and Tang, 1993). The micro-droplets can be dried to a desired level before interacting with the x-ray beam. Ionization and dehydration can interfere with the conformation of the sample, and it is thus important to understand these processes in detail. It is known, for instance, that unfolding of proteins in vacuum is possible, especially when they are highly charged (Jarrold, 1999; Velazquez et al., 1999; Iavarone and Parks, 2005). It is also known, that conditions exist under which unfolding does not take place (Tito et al., 2000). In a recent paper, Patriksson et al. (2007) have shown that it is sufficient to have a thin water layer (consisting of only a few water molecule) around the protein to maintain the solvent structure in the gas phase.

Both Bergh et al. (2004) and Hau-Riege et al. (2004) predict that clusters exposed with an XFEL pulse will explode in shells, where outer shells expand very fast compared to the rest of the cluster due to higher net charge, leaving an inner core, which is initially nearly stationary. This leads to the idea of keeping sample molecules in a protecting water cluster, not only because its is an efficient way to deliver the sample to the x-ray beam, but also to help with slowing down the explosion of the molecule of interest, which might be necessary.

4.1 Studies on water droplets in vacuum

In Papers 3 and 6 the evaporation process from pure water clusters and water clusters containing different ions is studied. An understanding of the dynamics of the sample under vacuum conditions requires some ideas about expected structural and thermal changes in the surrounding solvent during the evaporation process. In agreement with expectations, our results show that evaporation is highly temperature dependent. As water evaporates, it drains the remaining system of kinetic energy, and the droplet cools down. Simulations performed on clusters ranging from 125-4096 molecules show that once the temperature reaches 240 K, the evaporation slows down significantly. For neutral water clusters, starting at temperatures of 250 K, 275 K and 300 K, the temperature seems to converge towards 215 K for all simulated cases. At 215 K, the evaporation has almost completely ceased. From these results the number of evaporated water molecules from clusters starting at 275 K is estimated to be around 1 per nm^2 of the surface area. Compared to macroscopic droplets generated by aerosol techniques the simulated systems are much smaller. Nevertheless the results are promising, in the respect that they show the same temperature and evaporation tendencies for all simulated cluster sizes.

By extrapolating the results to larger systems, one can predict that a neutral cluster of 8000 molecules (with a diameter of around 10 nm) would not decrease its radius with more than 0.3 nm. Combining the knowledge about evaporation from water clusters in vacuum with the studies of biomolecules surrounded by a few layers of water (Patriksson et al., 2006), gives us valuable information about sample handling. This knowledge is important for the success of the single molecule imaging project.

In reality, water droplets are seldom neutral. This directed us to study the effect of ions on the evaporation. Paper 6 describes calculations on water clusters (up to 512 molecules) doped with 3-8 singly charged ions (Na^+, NH_4^+, Cl^- and $H_2PO_4^-$). The results show similar evaporation and temperature rates to rates in pure water clusters, but in the clusters containing Na^+ or Cl^-, the evaporation is slowed down slightly. This is caused by the fact that these ions tend to locate themselves close to the cluster surface. The relation between ion content and evaporation rate is not trivial, and requires further investigations. The picture that emerges form studies on the four test ions suggests that the radial position of these ions within the cluster affects evaporation rates.

The Rayleigh limit for spherical droplets (Rayleigh, 1882),

$$q^2 = 64\pi^2\epsilon\sigma r^3, \tag{4.1.1}$$

(where q is the number of charges that can be contained within the droplet, ϵ the permittivity of the medium surrounding the droplet, σ the surface tension of the liquid r the radius of the sphere) is known to overestimate

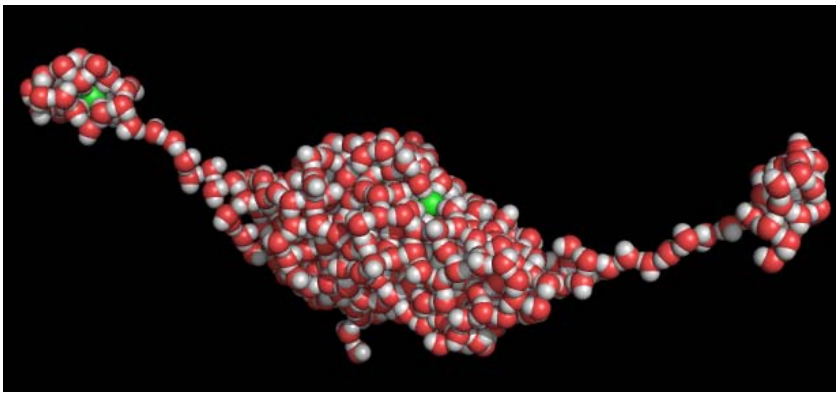

Figure 4.1: A water cluster containing four Cl^- ions and 210 water molecules being ripped apart due to the Coulomb forces between the ions. The Cl^- ions are green in the picture.

the maximum number of charges in a stable nanoscale system (Marginean et al., 2006), which our simulations verify. In simulations, the surface tension is underestimated, and different water models show quite different surface tension values. In bulk SPC water, the surface tension is 59×10^{-3}N/m (Abbas et al., 1995), compared to the experimental value 72×10^{-3}N/m (Weast, 1977). It is also known that the surface tension depends on the size of the simulated cluster (Zakharov et al., 1998). In the case of the two anions, the Rayleigh limit seems to give a better estimation of the maximum charges than in the case of the positive ions. This was found to be related to the hydration energy (Marcus, 1994), and to the ion-ion structure within the water cluster.

In clusters that carry more charges than the Rayleigh limit, the ions rip the cluster apart, resulting in smaller satellite clusters, containing only a few ions below the Rayleigh limits. Figure 4.1 shows a water cluster containing Cl^- above the limit, being ripped apart. The simulations do not reveal any significant structural changes in the water. At temperatures well below 0 ˚C, it is tempting to believe that the water forms structured ice. However, experiments have shown that structural transitions from water to structured ice (in contrast to amorphous ice) in small droplets occurs at temperatures below 200 K (Huang and Bartell, 1995; Bartell and Huang, 1994; Stein and Armstrong, 1973), and our clusters never reach temperatures below 210 K. To simulate the transformation from the amorphous phase to the structured ice using MD have proven to be hard. Successful simulations on freezing water into crystalline ice are rare, and these have not been done under natural conditions (Matsumoto et al., 2002; Svishchev and Kusalik, 1994; Zangi and Mark, 2003). Evaporation, on the other hand is something that is well described by MD, and the simulations presented in Paper 3 are in good

agreement with a phenomenological expression for the evaporation, based on experimental results (Tang and Kebarle, 1993).

5. Interaction of photons with material

To understand what happens to a microdroplet, a cell, a sample molecule when it meets the FEL pulse, we need to comprehend photon material interaction.

X-rays interact with matter through absorption and scattering. As mentioned in the introduction, one of the limiting factors concerning structural studies using intense x-ray sources is the damage of the sample due to absorption.

In photo absorption, the energy of the photon is transferred to an electron, which is then ejected from the atom, leaving a positively charged ion behind. This is the main process that leads to damage in the sample.

Photon scattering can either be elastic, where the photon energy is conserved, or inelastic, where some of the photon energy is transferred to the atom. Generally, elastic scattering contributes to the recordable information in the diffraction pattern, while inelastic scattering does not carry easily decipherable structural information.

Inelastic scattering is a relatively rare event at x-ray frequencies although it is the main source of energy deposition with hydrogen, and represents about 3% of all interactions between x-rays and a biological sample at 1 Å wavelength. During inelastic scattering, the incoming photon excites an electron to some virtual level and when the electron relaxes emitting a photon, it does not come back to the ground state. The photon emitted has therefore a different frequency from the photon absorbed, and it also has an altered phase. When the photoelectron ejected from a core level leaves behind a vacancy, an electron from a higher energy level may fall into the empty orbit, resulting in a release of energy. This energy may be emitted in the form of a photon (dominant process with high-Z elements), but it can also be transferred to an outer shell electron which is then ejected from the atom in a process called Auger decay (Auger et al., 1939). The Auger electron carries the kinetic energy corresponding to the difference between the shell binding energy and the energy of the initial electronic transition, as illustrated by Figure 5.1. Compared to the photoelectron generated by an x-ray photon, the energy of the Auger electron is significantly lower, and it is ejected at a later time than the photoelectron. In biologically relevant material Auger electrons have energies between 250 eV-2 keV (Thompson

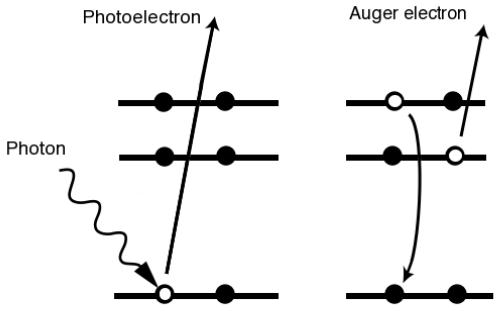

Figure 5.1: The Auger decay. This is one of two principal processes for the relaxation of an inner shell electron vacancy in an excited or ionized atom. The Auger effect is a two electron process in which an electron makes a discrete transition from a higher shell to fill a vacant inner shell hole. The energy gained in this process is transferred to another bound electron which then escapes from the atom. This outgoing electron is referred to as an Auger electron. The photoelectron and the Auger electron are released at different times, and have different energies. The figure on the left shows a high energy photoelectron leaving the inner shell. The figure on the right shows the release of the low energy Auger electron as the system relaxes. Auger decay is the dominant relaxation process for filling K-hole vacancies in light elements, like C, N, O, S, P.

and Vaughan, 2001), compared to the photoelectron carrying the energy of the incoming photon minus the shell binding energy (typically between 3-20 keV with x-rays). The physics of this decay is well understood (Hubbell et al., 1975; Veigele, 1973).

The life time of the inner level vacancy can be determined by measurements of the Auger line widths (Krause and Oliver, 1979). For atoms abundant in biological samples (such as C, N, O and S), the K-hole lifetimes are up to around 10 fs. During the photoionization process, the photoelectron may interact with valence electrons, leading to the so called shake-up and shake-off effects (Siegbahn et al., 1969). For light elements of biological significance, electrons emissions from these effects are in order 10-30% of the events where a low energy electron (10-100 eV) is emitted (Persson et al., 2001).

5.1 Secondary electron cascades

As atoms are photo-ionized, the electrons ejected from the atom will interact with the surrounding sample. In a macroscopic sample, both the pho-

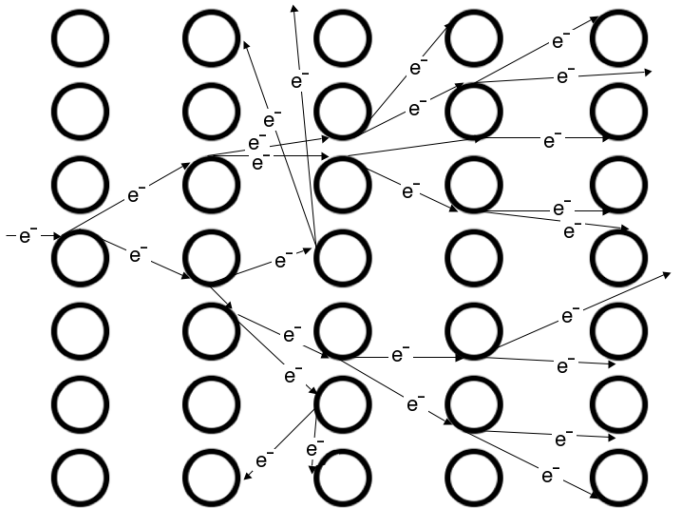

Figure 5.2: Secondary electron cascades. The initial electron, emitted through the Auger decay, leads to an avalanche of electrons due to inelastic scattering.

toelectrons and the secondary Auger electrons become thermalised and trapped inside the sample. Thermalisation is based on inelastic electron-electron interactions and, to a lesser degree, on electron-nuclear interactions. An electron scattering inelastically on an atom may cause a second ionization of an outer shell electron. This mechanism leads to an avalanche of electrons generated from one single photoionization event, as illustrated by Figure 5.2. Thermalisation produces a large number of such secondary "cascade electrons" (Ziaja et al., 2001, 2002, 2005). The number of these cascade electrons is roughly proportional to the energy of the impact electron triggering the cascade. These electrons are redistributed in the sample and can recombine with atoms. On the ~100 fs time scale, considered relevant to damage formation in single molecule imaging, the recombination is probability very low (Landau and Lifschitz, 1977). Collisions with atoms are highly relevant for the understanding of x-ray induced damage.

Paper 1 describes secondary electron cascades generated from an Auger decay in water (Auger energy for oxygen in a water molecule is 507.9 eV (Wagner et al., 1980)). The goal is to map the characteristics of electron cascades to support further development of the model used by Neutze et al. (2000), where the effects of the secondary ionization was not included. The studies of radiation damage in water are highly relevant, since water has a density comparable to that of biosamples and it has

been predicted that water would be used a carrier liquid containing the samples as they are exposed to the x-ray pulse. The calculations show that the number of electrons generated from a single Auger decay in liquid water is around 20. The thermalization of the secondary electrons through collisions occurs after only a few femtoseconds.

The results were later used by Bergh et al. (2004), where electrons where incorporated into a classical MD scheme as a continuous electron gas. In the electron gas model the electrons are assumed to thermalize immediately, compared to atoms, and can therefore be regarded as Maxwellian. Conclusions drawn from Bergh et al. (2004) show that free electrons in the sample shield positive charges on the ions, and slow down the explosion.

Our computational results give around 20 electrons per Auger decay in water (energy of Auger electron from oxygen: 507.9 eV), and this is in good agreement with results from radiolysis experiments on water (Muroya et al., 2002) where around 25 electrons are detected per 500 eV of an initial electron. The time scale of the experiments is much longer than in our calculations. It is therefore expected that effects not included in the model, such as recombination, should be relevant. Still the fact that experiments and theory agrees is ensuring.

5.2 Calculations of electron inelastic cross sections

The calculations of secondary electron cascades in materials, presented in Papers 1 and 5, use empirical models based on optical data to calculate the inelastic cross sections for electron scattering on atoms. Two different models, the Ashley model (Ashley, 1990, 1991) and the Tanuma, Powell and Penn model (TPP) (Penn, 1976, 1987; Tanuma et al., 1988, 1991a,b, 1993a,b) were employed in Paper 1.

Calculations based on the Ashley model are believed to underestimate the number of electrons generated (Ziaja et al., 2005), therefore only the TPP model was used in the studies described in Paper 5.

Silkin et al. (2003) have presented first-principles calculation of the electron inelastic mean free path in beryllium metal. They used the so called GW[1] approximation (Hedin, 1965) of the Density Functional Theory (DFT) (Kohn and Sham, 1965).

For cross sections of electron scattering of free atoms, a couple of analytical expressions, adapted to fit experimental data, are also available, see for example (Lennon et al., 1988) and (Kim and Rudd, 1994). For cross sections in solids, two different methods have been employed in this thesis. Both follow an approach developed by Fermi (Fermi, 1924; Bethe, 1930) where the passage of a fast charged particle is treated through the linear pertur-

[1] G stands for Green's function, W for the screened potential.

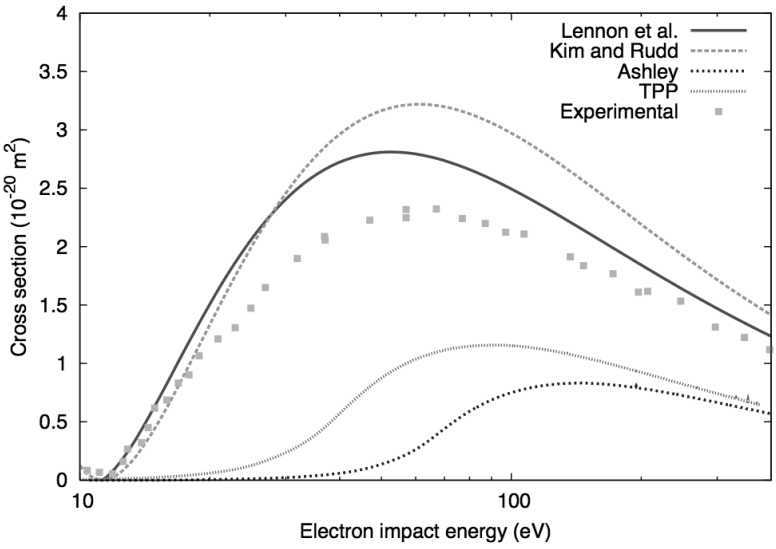

Figure 5.3: Electron impact ionization cross sections for carbon. Kim and Rudd (1994) is a semi-empirical model for free atoms, with parameters used in the explosion dynamics calculations by Jurek et al. (2004b). Lennon et al. (1988) is another semi-empirical approach again for carbon, used by (Hau-Riege et al., 2004). Ashley and TPP are two solid state models, applied to diamond (Ashley, 1990; Tanuma et al., 1988). This was used in Papers 1 and 5, and the results were used in Bergh et al. (2004). Experimental data are from free atoms (Brook et al., 1978).

bation caused by its electric field in the solid. We used two models here (Ashley and TPP) together with the Lindhard dielectric function (Lindhard, 1954) to estimate the number of electrons generated. The models have different ways to compensate for the fact that the dielectric function is only known for photons, where the momentum transfer is zero. Ashley includes the exchange between the incoming electron and the electrons in the solid in accordance with the non-relativistic Møller cross section (Kaku, 1993). The TPP approach on the other hand, is developed for calculating inelastic mean free paths for electrons in a solid. Figure 5.3 illustrates the difference between the electron cross sections based on two semi-empirical free electron approaches (for carbon) and the two models for electron cross sections in solids, in this case diamond. As mentioned, the two models are dependent on the knowledge of the dielectric function, which typically have been taken from experimental data.

In Paper 5, a new strategy is presented and tested. The energy loss function was determined using GW calculations, and the secondary electron dynamics in two alkali-iodides were than calculated and compared to calcu-

lations based on experimental data (Creuzburg, 1966). We made a comparison of results based on the GW calculations and experiment, concluding that in the two test cases (KI and CsI) the calculations gave comparable outputs. This indicates that the energy loss function based on GW calculations can be used where no experimental data are available. The results are further discussed in Chapter 6.

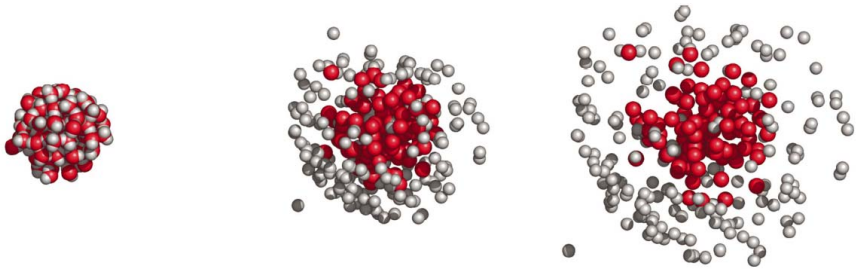

Figure 5.4: Water cluster exploding under the influence of a 15 fs XFEL pulse at 1 Å wavelength and with 10^{12} photons per pulse focused to a 100 nm diameter spot. Snapshots were taken at -10, 0 and 15 fs, with the pulse centered at t=0 fs. These snapshots are from Bergh et al. (2004), using results described in Paper 1. The dynamics of the explosion is influenced by the electron gas.

The hard x-ray damage calculations on bio relevant material including secondary electrons (Hau-Riege et al., 2004; Jurek et al., 2004b; Bergh et al., 2004) treat the generation of secondary electrons differently. Hau-Riege et al. and Jurek et al. use cross sections from free atoms to calculate the low energy productions, whereas Bergh et al. use electrons calculated in a solid state approach (snapshots from the calculations of Bergh et al. (2004) can be seen in Figure 5.4). Which of these approaches is better, depends on a whole range of factors. Generally the solid state approach is more accurate before the sample starts exploding, and the single particle approach is better to describe the explosion while it is happening. As Figure 5.3 shows, the difference between cross sections is large, specially at low energies, yet the damage studies using the different models (Hau-Riege et al., 2004; Jurek et al., 2004b; Bergh et al., 2004) give fairly similar results.

Ionization in the vacuum ultra violet (VUV) regime is significantly different from ionization in the hard x-ray regime (Ziaja et al., 2006). The high field limits with hard x-ray are very high, and multiphoton processes can be neglected with photon intensities expected from XFELs. Hard x-rays trigger inner shell processes. In contrast, absorption of a VUV photon causes ionization through outer shell processes. Samples exposed to a highly focused VUV FEL pulse experience multiphoton processes and inverse Bremsstrahlung is significant in the sample exposed to a focused

VUV pulse. As a result, photoionization is significantly different with soft x-rays than with hard x-rays. In a recent paper Ziaja et al. (2006), propose a model for describing ionization and ionization dynamics in the VUV regime, using Boltzmann equations. This model was successfully applied to describe the behavior of xenon clusters in a focused VUV pulse from the VUV-FEL, and the results showed qualitative agreement with experimental data.

6. Time resolved studies

Ultrafast phenomena are typically studied using pump-probe techniques where the dynamics are initiated by an ultrafast laser (the pump pulse) and probed after some time with a second pulse (the probe pulse). If the probe pulse originates from a high harmonic laser source, the pump pulse and the probe pulse can both be generated from the same source, using a delay line which creates different optical path lengths for the two pulses. In such cases, the time resolution is limited by the overlap of the pump pulse with the probe pulse, and can be less than a femtosecond (Hentschel et al., 2001).

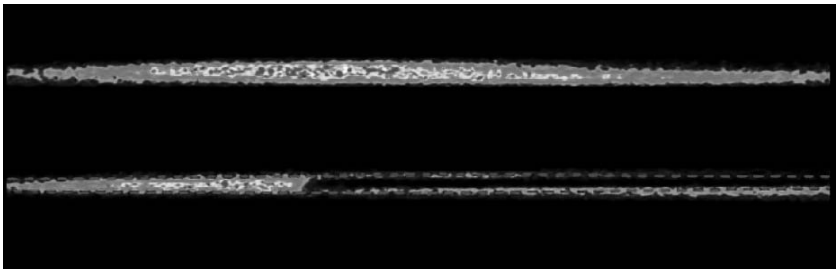

Figure 6.1: Demonstration of the principle of measuring the time delay between pump and probe by after the experiment is carried out. Cross beam geometry (Hajdu, 1994; Neutze and Hajdu, 1997; Synnergren et al., 2002); the upper picture is the x-ray diffration form the unperturbed InSb crystal, in the lower picture the laser pulse have reached the sample and melted the crystal such that it does not diffract any longer (the dark line). The experiment shown was performed at SPPS, by Jörgen Larsson and coworkers.

At a typical accelerator based x-ray source, the pump and the probe pulses come from different sources. Timing jitter (a random time delay) between the pump and the probe pulses affects temporal resolution, and synchronization of these pulses becomes a primary concern in ultrafast time-resolved studies. Requirements for tight synchronization can of course be relaxed in studies of slower processes. This was the case for experiments presented in Paper 2, where recrystallization was followed over nanoseconds, and speed was primarily limited by the detection system.

A way to reduce the problem of jitter at accelerator-based light sources is offered by measuring it. This can be done by electro optical sampling (EOS), a method developed at SPPS by Cavalieri et al. (Paper 7). EOS measures the arrival time of each high energy electron bunch to the undulator. The arrival time of each x-ray pulse can this way be determined relative to an external laser pulse. Results from SPPS show time resolutions better than 60 fs rms. EOS is thoroughly explained in the reference.

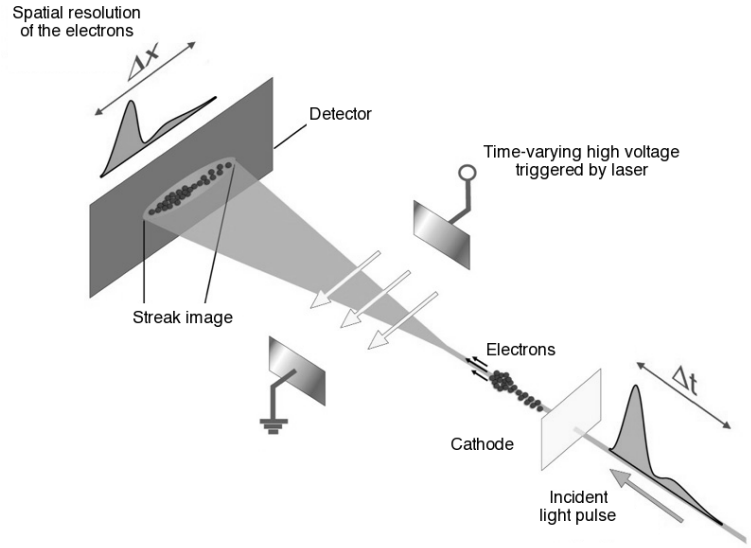

Figure 6.2: Layout of a conventional streak camera. Image reproduced with permission from The Max Planck Institute for Quantum Optics/Vienna University of Technology.

A second way to handle the jitter is to deal with it after the experiment is completed, simply by interpreting the read out from the detector. By knowing the pulse lengths and the geometry of the two sources, the timing can be determined by analyzing the data, using the so called crossed-beam topography geometry (Hajdu, 1994; Neutze and Hajdu, 1997; Synnergren et al., 2002). Figure 6.1 illustrates this approach, which was applied in the experiments presented in Papers 8, 9 and 10. By crossing the pump and probe beams on the sample and imaging the diffracted x-rays, one can map the temporal information into spatial information, enabling collection of the complete time history around time zero in a single shot. In the figure, the x-ray pulse is diffracted by an InSb crystal. The laser pulse melts the crystal, and where the sample melted it does not diffract. Hence the dark line in the melted area of the crystal.

A more well established way to measure the delay between the pump and the probe can be done by using a streak camera (Key et al., 1980). Figure 6.2 shows the layout of a conventional streak camera. The x-ray photons hit the cathode, where they generate an electron bunch that is accelerated towards a detector. These electrons are exposed to a high voltage electric field that is triggered by the laser pulse. This results in an image on the detector where the overlap of the two pulses can be interpreted by the spatial spread of the streak image. One of the main parameters that affect the time resolution is the ability of the cathode to generate electrons rapidly with a narrow energy and spatial distribution (Lowney et al., 2004).

Paper 5 provides a purely theoretical study on the development of secondary electron cascades in two photocathode materials (KI and CsI). These studies employed a method described in Paper 1 (further explained in Chapter 5). This method allowed us to explicitly follow electron trajectories, which was not possible in earlier investigations. Both materials are stable, and possess good photocathode properties (Verma, 1973). They were also studied earlier experimentally (Lowney et al., 2004; Henke, 1972) and theoretically (Kane, 1966; Henke et al., 1979). Our simulations consider impact electrons with a kinetic energy of 500 eV, and the results show that both materials release a similar number of secondary electrons. The number of electrons liberated by electron cascades seems to saturate slightly faster in CsI than in KI, but KI shows a significantly narrower secondary electron distribution than CsI. These characteristics indicate that a streak camera with a KI photocathode could give a higher temporal and spatial resolution than a streak camera a CsI with photocathode.

7. Laser induced phase transitions

This chapter summarizes results on laser induced structural transitions reported in Papers 2 and 4.

7.1 Thermal phase transitions

Heating a material makes atoms vibrate. If the added energy is large enough, the material may go through a phase transition into a lower ordered state. In a solid, the free energy is defined as the $F = U - TS$, where U is the internal energy of the system, T the temperature and S the entropy (Kittel, 1996). When two phases (L and H) are allowed at the same temperature, T_C, such that $F_L(T_C) = F_H(T_C)$, the material may change from its higher structured order phase to a lower order phase.

7.1.1 Laser induced melting of ice studied by MD

In classical MD simulations electrons are not considered explicitly. As long as the system is not ionized, structural changes induced by an external electric field can still be studied. Furthermore, MD is an eminently suitable tool to do so, since it gives the exact position of each atom at every time step. As mentioned in Chapter 3, the choice of molecular model (in this case the water model) is crucial for the result of a simulation. In the study presented in Paper 4, we used a water model developed to reproduce IR absorption. The model (flexible TIP4P by Lawrence and Skinner (2003)) includes a Morse potential (Morse, 1929) to describe oxygen-hydrogen vibrations. The Morse potential is described as

$$V(r) = D_e[1 - e^{-a(r-r_e)}]^2, \tag{7.1.1}$$

where r is the distance between the atoms, r_e is the equilibrium bond distance, D_e is the well depth (defined relative the dissociated atoms) and a is a constant controlling the width of the potential.

The simulations presented in Paper 4 provide a deeper understanding of experimental results on ultrafast superheating of ice performed by Iglev et al. (2006). We find that when heating ice to temperatures above 290 K with a short pulsed IR laser, the ice stays in a super-heated state for only a

few picoseconds before melting, whereas upon heating to T<290 K the system can stay superheated for nanoseconds. In the latter case the melting of the crystal structure did not show a linear dependence on the amount of energy deposit in the system, but seemed to be governed by a statistical process. We found that thermal melting follows a nucleation process, where the break down of the ice structure starts at highly localized points and spreads out through the crystal. Pockets of intact crystalline structures could be found a couple of picoseconds after the melting process had been initiated.

The upcoming hard x-ray FELs will provide a revolutionary experimental tool to study rapid structural transitions, such as melting of ice using a short-pulse laser. Simulations, as those presented in Paper 4, serve as a useful guideline in the design of future experiments.

7.2 Non-thermal melting

In a non-thermal melting process, the electrons and the crystal lattice are not in equilibrium. Equilibrium between the electrons and the lattice is established on a picosecond timescale, which corresponds to the typical timescale of the electron-phonon coupling. In such processes the concept of temperature breaks down, hence the free energy is not defined. To define a phase transition in such extreme cases the Lindemann criterion can be used (Lindemann, 1919). The Lindemann criterion states that when the atomic displacement reaches 10% of the nearest neighbor distance, the material melts. During laser induced non-thermal ultrafast processes the electron pressure and temperature can reach extremely high values, since these processes occur much faster than the typical phonon electron coupling time.

7.2.1 Time-resolved x-ray diffraction experiments

X-ray diffraction is a very sensitive instrument to determine the order of a sample and therefore it is an excellent probe for investigating phase transitions. Generally the x-ray diffraction efficiency is much higher for a crystalline sample than for an amorphous sample, which makes x-rays ideal for structure determination of crystals. Ultra short x-ray pulses permit high temporal resolutions in x-ray diffraction experiments. In the experiments presented in Papers 8, 9 and 10 the time resolution was set only by the x-ray pulse duration, achieving a resolution of around 100 fs.

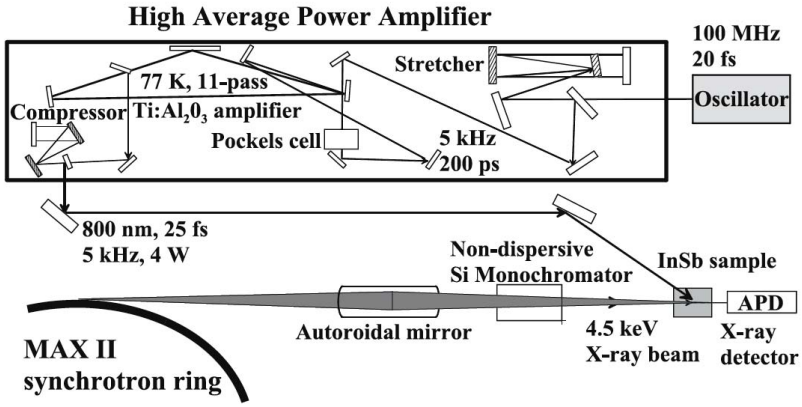

Figure 7.1: Experimental setup at the beam-line D611, MAX-lab

7.2.2 Resolidification of non-thermally molten InSb

Experiments described in Paper 2 were performed to investigate the crystal regrowth of ultrafast melted InSb. Experiments were carried out at the D611 beamline at the MAX-lab synchrotron radiation facility in Lund (Sweden). The general experimental set up is shown in Figure 7.1. An optical laser pulse (800 nm, 25 fs, < 55 mJ/cm^2) was used as the pump pulse, and the x-ray beam from the MAX II synchrotron ring was used as the probe pulse. This experiment required a temporal resolution of a few nanoseconds, and therefore, the laser was not locked to the radio frequency signal from the cavities of the synchrotron. Instead, the temporal resolution was given only by the detection system. This method is preferable in cases where low temporal resolution but long recording times are needed.

A requirement for the pump-probe experiments performed here is to match the penetration depth of the x-ray pulse with the penetration depth of the optical laser pulse. This could be achieved with an asymmetrically cut InSb wafer, such that the (1 1 1) plane was tilted 19˚towards the (1 1 0) direction.

The bandgap of InSb is 0.417 eV (Vurgaftmana et al., 2001) and the energy of the optical laser photons was 1.55 eV (800 nm), leading to direct ionization and non-thermal melting of the sample. The detected x-ray signal gives an intuitive understanding of the melting and resolidification process (Figure 7.2) where the recovering x-ray signal is a result of crystal regrowth.

In an x-ray experiment involving a pump laser, there are a number of factors that can smear out the detection signal, which in this specific case blur the distinction between the molten and crystalline phase. Semiconductors

that are irradiated repetitively lose diffraction efficiency. The extreme heating causes a pressure wave in the sample, leading to a deformation of the structure, which may cause epitaxial regrowth (Perez and Lewis, 2003). Decomposition of the InSb crystal takes place in the molten phase, and Sb evaporates faster than In (indium) due to a higher vapor pressure, and this leades to a shortage of Sb in the sample.

These effects result in a non-perfect regrowth, and induce a higher mosaicity in the sample than in the unperturbed case. Thermal vibration of the atoms is an other factor that reduces the intensity of the diffracted x-rays. This effect can be described by a Debye-Waller factor (Warren, 1990). In InSb at 500 K thermal effect reduce the intensity by about 5% compared to 300 K (Kushwaha, 1981). The Debye-Waller effect and the increase in mosaicity can clearly be seen in the data, which show a broader rocking curve and a lower diffracted intensity (Figure 7.2).

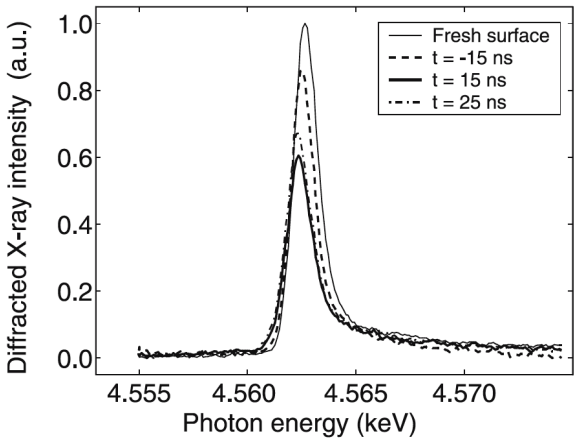

Figure 7.2: Energy-scans at different time delays. The thin solid line corresponds to a sample surface before laser irradiation. The rocking curve under static laser conditions can bee seen as the dashed curve. It was measured during irradiation, in between pulses, 15 ns before the next laser pulse arrived. The thick solid line is measured with a 15 ns probe delay with respect to the laser pulse. Further reduction in diffraction efficiency is observed. This is due to x-ray absorption in the molten sample material. The dash-dotted line recorded at 25 ns delay shows recovery of the diffraction efficiency, which is due to regrowth of the crystal structure.

The massive increase in the free-carrier density is due to the heavy ionization caused by the optical laser. This changes the optical properties of the sample, including reflectivity and the index of refraction. This can be modeled by the Drude model (Drude, 1900). The electron-hole recombination can be ignored in the early steps, since these take place on a nanosecond timescale (Landau and Lifschitz, 1977) and the laser pulse length is on the

order of femtoseconds. In this approximation the total refractive index due to the free electrons is given by

$$n = n_0 \sqrt{1 + (\frac{\omega_\mathrm{p}}{n_0 \omega})^2 (-1 + i \frac{1}{\omega \tau_\mathrm{e}})}, \tag{7.2.1}$$

where n_0 is the complex lattice index of refraction, ω_p the plasma frequency, ω the laser frequency and τ_e the electron collision time. From Equation 7.2.1 it follows that the electron plasma acts as a mirror at the plasma frequency, when $\omega_\mathrm{p} = n_0 \omega$. Since the plasma frequency is dependent on the number of free charge carriers, it is complicated to calculate the reflectivity during the laser radiation. The ionization of the sample is not proportional to the laser fluence, due to multi-photon ionization and electron impact ionization, which both make the reflectivity hard to model. For studies of regrowth as presented in Paper 2, knowledge of the reflectivity is not crucial. However, the damage aspect is interesting, and measuring the change of reflectivity in the sample is a way to determine the number of free electrons through the Drude model. This could be a way to perform experiments that could support, or overthrow, the secondary electron cascade calculations presented in Papers 1 and 5, as well as (Ziaja et al., 2001, 2002, 2005), where few affirmative experiments are yet available.

8. Outlook

The impact of imaging non-crystalline samples at high resolutions is widely expected to be substantial in a broad range of sciences and technologies. Advances made here have the potential to revolutionize structural studies in many disciplines of science, similar to what synchrotron radiation once did. Experimental verification of the principle of single molecule diffraction imaging has now been performed. This was done at the first soft x-ray FEL in the world, the FLASH facility at DESY in Hamburg. Experiments performed at FLASH taught us much about image reconstruction, sample handling, and the damage caused by intense soft x-ray pulses. The results fully support predictions, and indicate that an interpretable diffraction pattern can be obtained before the sample turns into a plasma as a consequence of an exposure to an extremely intense and very short soft x-ray pulse. This provides the first experimental proof for the basic principle of single molecule imaging, showing that one can get an interpretable diffraction pattern before sample explosion. The results have implication for imaging non-periodic molecular structures in biology and in any other area of science and technology where structural information on the nanoscale is valuable.

Atomic resolution structural studies will require hard x-rays. LCLS, the first hard x-ray free-electron laser, will become operational in 2009, and will produce intense hard x-ray pulses with wavelengths reaching about 1.0 Å. This XFEL will enable us to perform structural studies on single viral particles or on large macromolecules at or near atomic resolutions for the first time. We will also be able to test theoretical predictions for radiation damage with hard x-rays, leading to a deeper understanding of the damage process and refinement of the theoretical models.

Studies on the behavior of the sample in vacuo are guiding the development of novel procedures and instruments for sample injection. For this end, it is necessary to gain a deeper understanding of the behavior of biomolecules when injected into the vacuum chamber, and to understand and predict structural changes. There are a number of open questions here, and these will require attention.

An important aspect of the single molecule imaging project is the fact that it is multifaceted. One example of this relates to studies on structural transitions in water, and certain aspects if this are presented in this thesis. The

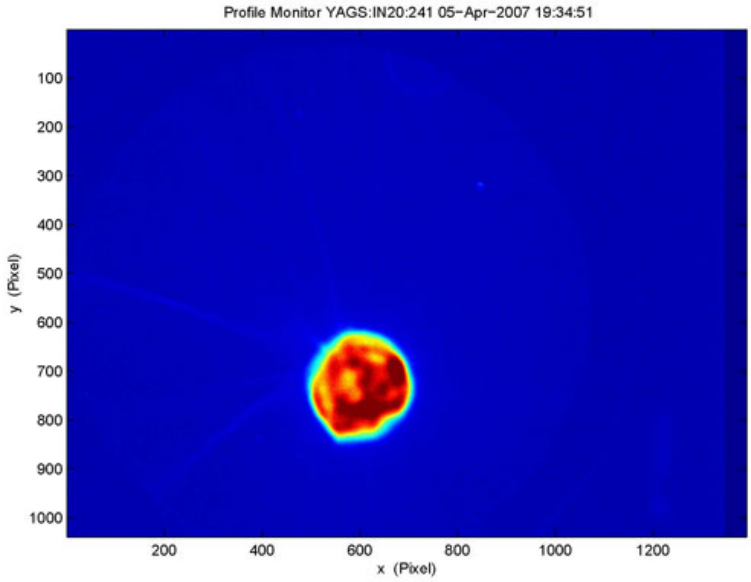

Figure 8.1: The first photo-electron beam produced by the LCLS injector on April 5, 2007 (www-ssrl.slac.stanford.edu/lcls/). The image shows the beam on a diagnostic viewer approximately 80 cm from the electron gun. Beam energy is 5.5 MeV, pulse length is 6 ps. This a first step towards the first hard x-ray FEL in the world.

hard x-ray FEL will provide just the right tool to experimentally investigate fast structural changes induced by photons, and give us a deeper knowledge of the properties of the most important liquid on Earth - water.

An example of an exciting spin-off of the single molecule imaging project is the prospect of obtaining nuclear fusion with FEL radiation. From damage modeling for biomolecule imaging, it emerged that protons could be accelerated to keV energies under certain conditions (Carlson, 2006). Biological imaging with XFEL is at the front-end of high-energy density science, and spin-off are bound to appear and give rise to exciting new areas of research in natural sciences.

We can only speculate about the future possibilities of single particle imaging. Everything has worked so far, but will it work all the way? And if it does work all the way, and we have refined the method and reached atomic resolution, where do we go next? Femtosecond time-resolved imaging of the chemical processes? High-resolution structures of cells? Pump-probe experiments on photosynthesis in situ?

This is the first thesis from the project on single molecule diffractive imaging, and it shows that some parts of the big puzzle are fitting together, and the motif that is appearing is really starting to look promising!

9. Sammanfattning på svenska

För att kunna förstå hur någonting fungerar är det en stor fördel att veta hur det ser ut. Detta gäller såväl i en klocka som i människokroppen. Ett stort område inom biokemi är därför strukturbiologi, inom vilket man försöker bestämma hur viktiga biomolekyler ser ut och hur de fungerar.

Idag strukturbestäms biomolekyler till stor utsträckning med hjälp av en teknik som heter röntgenkristallografi. Tekniken bygger på att molekylen som ska strukturbestämmas, till exempel ett protein, kristalliseras så att ett stort antal identiska molekyler sitter ordnade i ett tredimesionell mönster så att de bildar en kristallstruktur. Kristallen placeras i en röntgenstråle från en synkrotronanläggning och en diffraktionsbild av kristallen genereras. I det ideala fallet innehåller denna bild all nödvändig information för att strukturbestämma molekylen.

Att utsätta ett material för röntgenljus medför att man joniserar det. Genom att fotonerna i röntgenpulsen slår ut elektronerna runt atomkärnorna joniseras dessa. I ett starkt joniserat prov förstörs molekylstrukturen på grund av de krafter som uppstår mellan de laddade jonerna. Då man använder sig av en kristall blir effekten av joniseringsskadan inte så allvarlig. Detta beror på att skadan sker slumpmässigt över ett stort antal molekyler och diffraktionsbilden är ett medelvärde över dessa molekyler.

Flera av stegen i röntgenkristallografi är svåra, och ibland omöjliga, att utföra. Ett av de största problemen är att det är svårt att kristallisera många typer av biomolekyler. En teknik som tillåter strukturbestämning utan kristallisering skulle således vara till stor nytta.

Det har förutspåtts att det med hjälp av en mycket kort och intensiv röntgenpuls kan vara möjligt att generera en diffraktionsbild från, och därmed också strukturbestämma, ett icke-kristallint prov. Vill man undvika kristalliseringen måste man dock hitta ett sätt att komma runt problemet med att röntgenjoniseringen förstör molekylstrukturen. Idén är att om pulsen är tillräckligt kort kommer hela pulsen att kunna passera provet innan det exploderar på grund av joniseringen. Man kan se det som att man använder sig av en kamera med väldigt kort slutartid: vill man fotografera ett föremål i rörelse gäller det att använda en slutartid som är så kort att föremålet inte hinner röra sig såmycket att bilden blir suddig. Figur 5.4, i kapitel 5 illustrerar en vattendroppe som joniseras av en kort röntgenpuls. Om pulsen hinner gå igenom provet innan det explodera

(bilden till vänster) får man en tydlig bild. Använder man sig istället av en längre puls kommer bilden att bli suddig.

Idén om strukturbestämning av icke-kristallina molekyler med hjälp av korta röntgenpulsar är bakgrunden till denna avhandling. Möjligheten att kunna strukturbestämma vilken biomolekyl som helst skulle kunna få en enorm betydelse för biokemin och i förlängningen för den medicinska vetenskapen. Det är ett stort projekt att utveckla en teknik vilken gör strukturbestämning av molekyler utan att kristallisering möjlig. En hel rad problem återstår innan vi kommer att kunna lösa den första molekylstrukturen. Bild 1.1 illustrerar hur det tänkta experimentet skulle kunna gå till.

Vad denna avhandling presenterar är ett par pusselbitar, vilka kommer att bidra till den slutgiltiga förståelsen för hur en sådan metod skall fungera. Två områden inom ämnet presenteras i denna avhandling: hantering av biomolekyler i vakuum och fotoners (från röntgen- eller laserkällor) påverkan på materia.

För att kunna genomföra strukturbestämning av icke-kristallina molekyler behöver man leverera provmolekyler från en buffertlösning till röntgenstrålen på ett kontrollerbart och repetativt sätt. Eftersom allt som kommer i röntgenljusets väg bidrar till diffraktionsbilden, utförs diffraktionsexperimentet i vakuum. Ett sätt att leverera prov från lösning in i vakuum är att använda sprayteknik, vilket innebär att man sprayar små droppar som innehåller provet (molekylen) innesluten i buffertlösning, t.ex. vatten.

Att använda en sådan teknik har flera fördelar. Dels är det troligt att vattendroppen mer liknar molekylens naturliga miljö än vad vakuum gör. Dels har teoretiska beräkningar visat att ett omslutande vattenlager skulle kunna ha en fördröjande effekt på explosionen orsakad av joniseringen. Två delarbeten inkluderade i denna avhandling (artikel 3 och 6) undersöker hur små vattendroppar beter sig i vakuum. Detta är intressant eftersom förändringar i det omslutande vattnet även påverkar molekylen. Våra resultat visar att avdunstningen från dropparna sänker temperaturen (eftersom det är de varma vattenmolekylerna i vatten droppen som avdunstar). Då temperaturen sänks upphör avdunstningen. Detta innebär att man genom att veta temperaturen på vattendropparna då de sprayas in i vakuum kan förutspå hur mycket vatten som kommer att finnas kvar i provet då avdunstningen upphör.

Den typen av röntgenkälla, hårdröntgen-frielektronlaser, som behövs för att kunna strukturbestämma icke-kristalliserade molekyler, finns ännu inte tillgänglig. Två anläggningar är dock under konstruktion, en i Stanford i Kalifornien och en i Hamburg, Tyskland. Dessa kommer, om allt går enligt planerna, stå klara 2009 respektive 2013. Detta innebär att det hittills har varit svårt att utföra testexperiment för att kunna förstå vad som händer med ett prov då det placeras i en kort intensiv röntgenpuls. För att kunna

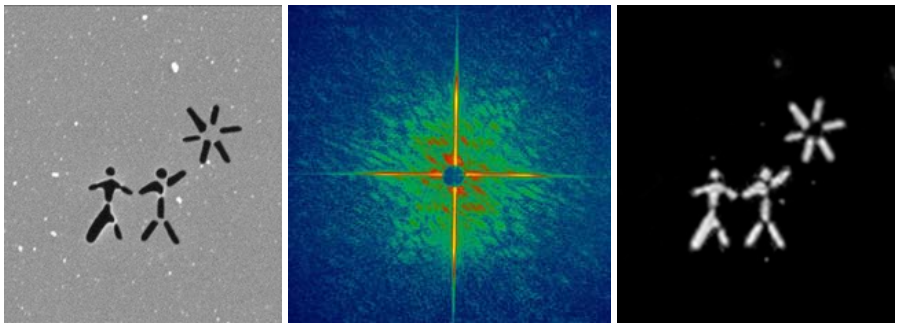

Figure 9.1: Demostration av pricipen att man kan återskapa en bild av ett föremål som förstörs p.g.a. röntgen pulsen som genererar diffraktions mönstret. Till vänster är orginal bilden, i mitten diffraktions bilden och till höger bilden skapad av diffraktions mönstret. Efter röntgen pulsen passerat igenom provet fanns ingenting kvar av det. Experimentet genomfördes vid FLASH i Hamburg (artikel 11).

svara på frågan hur kort en röntgenpuls måste vara för att hinna passera genom provet innan det exploderar, har vi därför hittills varit hänvisade till teoretiska beräkning och testexperiment vid röntgenkällor snarlika en röntgen-frielektronlaser. Fyra delarbeten i denna avhandling behandlar på olika sätt hur fotoner (från röntgenpulser eller laserpulser) påverkar materia, som till exempel ett bioprov.

Dessa delarbeten fokuserar dels på smältning med hjälp av laser och dels på jonisering initierad av röntgen. I det första fallet är kopplingen till icke-kristallin strukturbestämning inte helt självklar; det handlar mer om en allmän förståelse av strukturella förändringar i material på grund av laserstrålning. I delarbetet presenterat i artikel 4 har vi med hjälp av datorsimuleringar studerat hur is smälter på grund av påverkan av laserljus med olika energi, det vill säga smältningens våglängdsberoende, och på molekylnivå modellerat hur smältningen uppkommer och sprids i isen som slutligen blir vatten.

Artikel 2 är en experimentell studie av laserinducerad smältning av ett halvledarmaterial, indiumantimonid (InSb). InSb, som har en kristallin struktur på liknande sätt som vatten i sin fasta form, smältes med en intensiv laser och sedan studerades hur kristallen återbildades.

Som tidigare nämnts är det jonisering som leder till att strukturen av ett prov förstörs. Vill man veta hur fort detta sker, för att kunna avgöra hur kort puls som behövs, är det alltså väsentligt att förstå joniseringsprocessen. Två av delarbetena vilka presenteras här (artikel 1 och 5) beskriver jonisering till följd av röntgenstrålning. I denna joniseringsprocess slås en elektron ut ur sin bana runt atomen. Elektronen kan i sin tur jonisera en ny atom, varvid ytterligare en elektron slås ut, och så vidare (detta är schematiskt

illustrerat i figur 5.2 i kapitel 5). Denna kaskad av joniseringar (utlösta av elektroner) är en viktig del av den röntgeninducerade skadan i provet. Vi har gjort beräkningar på fyra testsystem kaliumjodid (KI) och cesiumjodid (CsI), samt is och vatten. Vatten och is valdes för att det har en densitet som liknar biomolekylers och för att vatten är, som tidigare nämnts, en potentiell provbärare i vakuum. KI och CsI valde vi för att de har relevans för en annan del av projektet, de är nämligen båda goda fotokatoder.

Våra beräkningar för KI och CsI visar resultat som pekar på att KI är en något bättre fotokatod för att nå en hög tidsupplösning. KI genererar nämligen elektroner med en smalare energifördelning, vilket är en viktig egenskap hos en snabb fotokatod.

För vatten visar våra resultat att varje röntgenfotonjonisering leder till 20 elektronjoniseringar. Vi ser också att elektronjonisering sker inom loppet av 0,1 ps[1]. Dessa resultat ligger till grund för beräkningar av hur kort röntgenpulsen måste om man ska kunna hinna ta en bild av molekylen innan den förstörs p.g.a. joniseringen. Resultaten pekar på att en puls kortare än 0,1 ps behövs för att det ska vara möjligt.

Hurvida våra beräkningar stämmer och vi en dag kommer att kunna lösa molekylstrukturer med hjälp av röntgen-frielektronlasrar får framtiden utvisa. De steg vi tagit hittills, av vilka denna avhandling är en del, visar alla att vi är på rätt väg. Vilken effekt möjligheten att kunna strukturbestämma icke-kristallina prov kommer att få på naturvetenskapen kan vi bara sia om. Kanske kommer vi i framtiden att kunna skapa bilder av celler med atomär upplöning? Eller i detalj kunna studera hur kemin i kroppen fungerar och på så sätt kunna skapa bättre läkemedel? Det enda vi vet säkert är att vi står inför en mycket spännande framtid.

[1] d.v.s. 0,0000000000001 sekund

Acknowledgements

It has been four years, eight months and twentysix days since I first entered the building known for its ugliness, BMC, and met Prof. J. Hajdu, who greeted me with an open hand and a smile, and said ”We need people with your experience and we’ve got money...”.

It has really been a privilege to work in a project as exiting as this and to be surrounded by such wonderful people. I would like to thank you all, those of you who supported me in science or in friendship or who just smiled at me in the BMC corridors or at the badge office. To make the acknowledgements chapter shorter than the thesis itself, I can not mention you all. However, by starting to thank the Swedish and the American taxpayers for financial support I guess I covered most of you. Nic once calculated how much of his paycheck that went into mine, and he concluded that it was not much to be thankful for, but that’s Nic.

So here we go. Time for the most read part of any thesis, but also the part that most authors spend the least time to write - since it is written hours before submission. Thank you for:

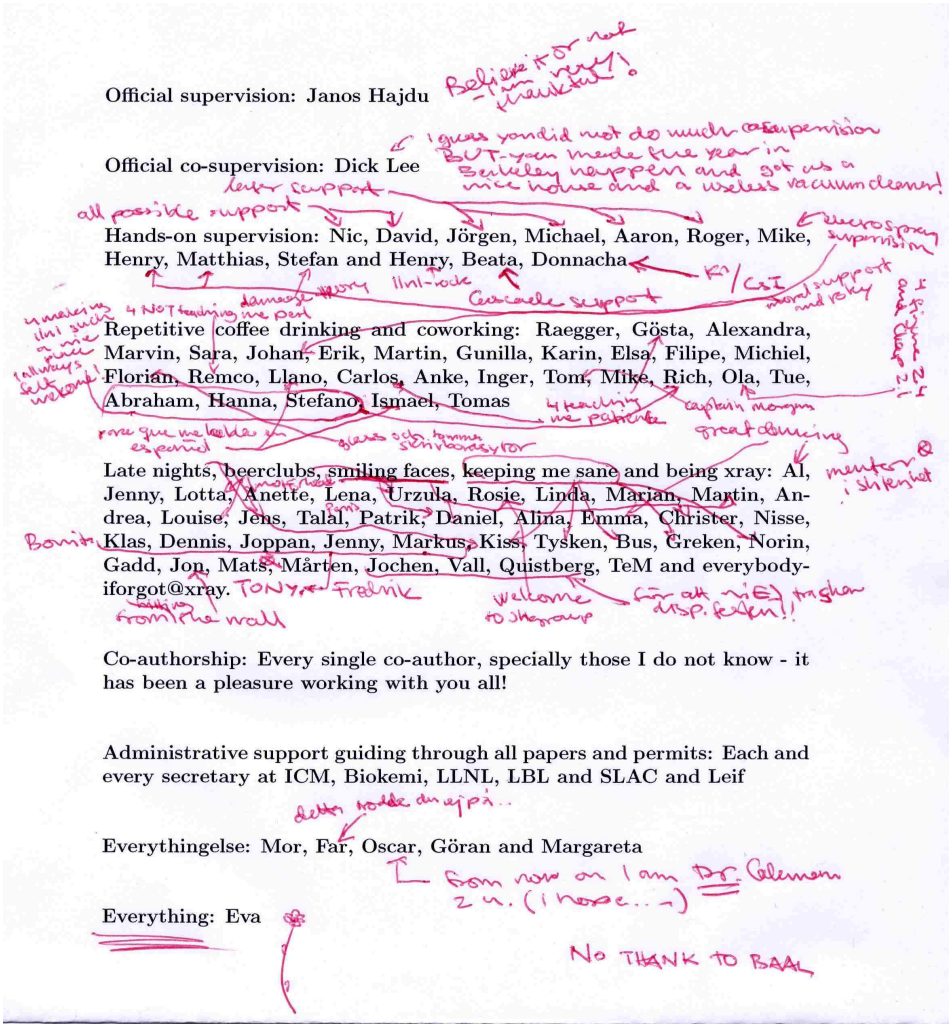

Official supervision: Janos Hajdu

Official co-supervision: Dick Lee

Hands-on supervision: Nic, David, Jörgen, Michael, Aaron, Roger, Mike, Henry, Matthias, Stefan and Henry, Beata, Donnacha

Repetitive coffee drinking and coworking: Raegger, Gösta, Alexandra, Marvin, Sara, Johan, Erik, Martin, Gunilla, Karin, Elsa, Filipe, Michiel, Florian, Remco, Llano, Carlos, Anke, Inger, Tom, Mike, Rich, Ola, Tue, Abraham, Hanna, Stefano, Ismael, Tomas

Late nights, beerclubs, smiling faces, keeping me sane and being xray: Al, Jenny, Lotta, Anette, Lena, Urzula, Rosie, Linda, Marian, Martin, Andrea, Louise, Jens, Talal, Patrik, Daniel, Alina, Emma, Christer, Nisse, Klas, Dennis, Joppan, Jenny, Markus, Kiss, Tysken, Bus, Greken, Norin, Gadd, Jon, Mats, Mårten, Jochen, Vall, Quistberg, TeM and everybody-iforgot@xray.

Co-authorship: Every single co-author, specially those I do not know - it has been a pleasure working with you all!

Administrative support guiding through all papers and permits: Each and every secretary at ICM, Biokemi, LLNL, LBL and SLAC and Leif

Everythingelse: Mor, Far, Oscar, Göran and Margareta

Everything: Eva

The author's contribution

Publications included in this thesis

Paper 1:

N. Tîmneanu et al. ***"Auger electron cascades in water and ice"***
I was deeply invloved in all parts of this project: planning, calulations, analysis and writing of the paper.

Paper 2:

M. Harbst et al. ***"Studies of resolidification of non-thermally molten InSb using time-resolved X-ray diffraction"***
This project was M. Harbst's and J. Larsson's idea and planning. It was my first experimental work and I was involved in the set up and performing of the actual experiment.

Paper 3:

C. Caleman and D. van der Spoel ***" Temperature and structural changes of water clusters in vacuum due to evaporation"***
This project originates from an idea of mine that D. van der Spoel believed in. I did almost all of the work.

Paper 4:

C. Caleman and D. van der Spoel ***"Picosecond Melting of Ice by an Infrared Laser Pulse"*** The idea for this project originates form an experiment we wanted to do at SPPS. I did all the simulations, most of the data analysis and most of the writing of the paper.

Paper 5:

C. Ortiz and C. Caleman ***"Secondary electron cascade dynamics in KI and CsI"***
During the work with Paper 1 I realized it was a limitation of the method to be dependent on experimental data. Talking to C. Ortiz I realized that he could provide calculated energy loss functions. At the same time I was asked about the secondary electron cascades in photo cathode materials, so we decided on performing the calculations. The work behind the final paper is equally divided between the authors, but my focus was on the electron calculations.

Paper 6:

C. Caleman and D. van der Spoel ***"Evaporation from water clusters containing singly charged ions"***
This is a continuation of Paper 3. I did all the simulations, most of the data analysis and most of the writing.

Supporting publications

Paper 7:

A. L. Cavalieri et al. ***"Clocking Femtosecond X Rays"***
I was at SPPS doing mainly other experiments and I help A. L. Cavalieri experimentally when that was required.

Paper 8:

A. M. Lindenberg et al. ***"Atomic-Scale Visualization of Inertial Dynamics"***
I was involved in the preparation and implementation of the experiment at SPPS.

Paper 9:

K. J. Gaffney et al. ***"Observation of Structural Anisotropy and the Onset of Liquid-like Motion During the Nonthermal Melting of InSb"***
Based on the same experiment as Paper 8, and my involvement in this paper was the same.

Paper 10:

J. Larsson et al. ***"Opportunities and challenges using short-pulse X-ray sources"***
Based on the same experiment as Paper 8, and my involvment in this paper was the same.

Paper 11:

H. N. Chapman et al. ***"Femtosecond diffractive imaging with a soft-X-ray free-electron laser"***
I was involved in the early stages of the sample preparations and the actual experiment.

Paper 12:

S. P. Hau-Riege et al. ***"Subnanometer-scale Measurements of the Interaction of Ultrafast Soft X-ray Free-Electron-Laser Pulses with Matter"***
I was involved in the preparation and execution of the experiment, and I was also somewhat involved in the writing process.

Paper 13:

S. P. Hau-Riege et al. ***"Damage threshold of inorganic solids under free-electron-laser irradiation at 32.5 nm wavelength"***
I was involved in the preparation and execution of the experiment, and I was also somewhat involved in the writing process.

Paper 14:

J. Chalupsky et al. ***"Characteristics of focused soft X-ray freeelectron laser beam determined by ablation of organic molecular solids"***
I was involved in the preparation and execution of the experiment.

Paper 15:

H. N. Chapman et al. ***"Femtosecond Time-Delay X-ray Holography"***
I was involved in the early stages of the sample preparations and the actual experiment.

Paper 16:

J. Chalupsky et al. ***"Ablation of organic molecular solids by focused soft X-ray free-electron laser radiation"***

This work is based on the same experiment as Paper 16. I was involved in the preparation and execution of the experiment.

References

Abbas, S., Ahlström, P., Nordholm, S., 1995. Molecular dynamnics simulations of surface tension for polar molecules. Correction for long-range interaction by generalized van der waals theory. Acta Chem. Scand. 49, 182–188.

Akre, R., Bentson, L., Emma, P., Krejcik, P., 2002. Bunch length measurements using a transverse rf deflecting structure in the slac linac. In: Garvey, T., Duff, J. L., Roux, P. L., Petit-Jean-Genaz, C., Poole, J., Rivkin, L. (Eds.), Proceedings of European Particle Accelerator Conference, 2002, Paris, France. CERN, Geneve, pp. 1883–1884.

Allen, M. P., Tildesley, D. J., 1987. Computer Simulations of Liquids. Oxford Science Publications, Oxford.

Andruszkow, J., Aune, B., Ayvazyan, V., Baboi, N., Bakker, R., Balakin, V., Barni, D., Bazhan, A., Bernard, M., Bosotti, A., Bourdon, J. C., Brefeld, W., Brinkmann, R., Buhler, S., Carneiro, J.-P., Castellano, M., P. Castro, L. C., Chel, S., Cho, Y., Choroba, S., Colby, E. R., Decking, W., Hartog, P. D., Desmons, M., Dohlus, M., Edwards, D., Edwards, H. T., Faatz, B., Feldhaus, J., Ferrario, M., Fitch, M. J., Flöttmann, K., Fouaidy, M., Gamp, A., Garvey, T., Gerth, C., Geitz, M., Gluskin, †. E., Gretchko, V., Hahn, U., Hartung, W. H., Hubert, D., Hning, M., Ischebek, R., Jablonka, M., Joly, J. M., Juillard, M., Junquera, T., Jurkiewicz, P., Kabel, A., Kahl, J., Kaiser, H., Kamps, T., Katelev, V. V., Kirchgessner, J. L., Körfer, M., Kravchuk, L., Kreps, G., Krzywinski, J., Lokajczyk, T., Lange, R., Leblond, B., Leenen, M., Lesrel, J., Liepe, M., Liero, A., Limberg, T., Lorenz, R., Hua, L. H., Hai, L. F., Magne, C., Maslov, M., Materlik, G., Matheisen, A., Menzel, J., Michelato, P., Möller, W.-D., Mosnier, A., Müller, U.-C., Napoly, O., Novokhatski, A., Omeich, M., Padamsee, H. S., Pagani, C., Peters, F., Petersen, B., Pierini, P., Pfülger, J., Piot, P., Ngoc, B. P., Plucinski, L., Proch, D., Rehlich, K., Reiche, S., Reschke, D., Reyzl, I., Rosenzweig, J., Rossbach, J., S. Roth, E. L. S., Sandner, W., Sanok, Z., Schlarb, H., Schmidt, G., Schümser, P., Schneider, J. R., Schneidmiller, E. A., Schreiber, H.-J., Schreiber, S., P. Schütt, . J. S., Serafini, L., Sertore, D., Setzer, S., Simrock, S., Sonntag, B., Sparr, B., Stephan, F., Sytchev, V. A., Tazzari, S., Tazzioli, F., Tigner, M., Timm, M., Tonutti, M., Trakhtenberg, E., Treusch, R., Trines, D., Verzilov, V., Vielitz,

T., Vogel, V., v. Walter, G., Wanzenberg, R., Weiland, T., Weise, H., Weisend, J., Wendt, M., Werner, M., White, M. M., Will, I., Wolff, S., Yurkov, M. V., Zapfe, K., Zhogolev, P., Zhou, F., 2000. First observation of self-amplified spontaneous emission in a free-electron laser at 109 nm wavelength. Phys. Rev. Lett. 85, 3825–3829.

Ashley, J. C., 1990. Energy loss rate and inelastic mean free path of low-energy electrons and positrons in condensed matter. J. Electron Spectrosc. Relat. Phenom 50, 323–334.

Ashley, J. C., 1991. Energy-loss probabilities for electrons, positrons, and protons in condensed matter. J. Appl. Phys 69, 674–678.

Auger, P., Ehrenfest, P., Maze, R., Daudin, J., Fréon, R. A., 1939. Extensive cosmic-ray showers. Rev. Mod. Phys. 11, 288–291.

Ayvazyan, V., Baboi, N., Bhr, J., Balandin, V., Beutner, B., Brandt, A., Bohnet, I., Bolzmann, A., Brinkmann, R., Brovko, O., Carneiro, J., Casalbuoni, S., Castellano, M., Castro, P., Catani, L., Chiadroni, E., Choroba, S., Cianchi, A., Delsim-Hashemi, H., Pirro, G. D., Dohlus, M., Düsterer, S., Edwards, H., Faatz, B., Fateev, A., Feldhaus, J., Flöttmann, K., Frisch, J., Fröhlich, L., Garvey, T., Gensch, U., Golubeva, N., Grabosch, H.-J., Grigoryan, B., Grimm, O., Hahn, U., Han, J., v. Hartrott, M., Honkavaara, K., Hüning, M., Ischebeck, R., Jaeschke, E., Jablonka, M., Kammering, R., Katalev, V., Khodyachykh, B. K. S., Kim, Y., Kocharyan, V., Körfer, M., Kollewe, M., Kostin, D., Krämer, D., Krassilnikov, M., Kube, G., Lilje, L., Limberg, T., Lipka, D., Löhl, F., Luong, M., Magne, C., Menzel, J., Michelato, P., Miltchev, V., Minty, M., Möller, W., Monaco, L., Müller, W., Nagl, M., Napoly, O., Nicolosi, P., Nölle, D., Nuñez, T., Oppelt, A., Pagani, C., Paparella, R., Petersen, B., Petrosyan, B., Pflüger, J., Piot, P., Plönjes, E., Poletto, L., Proch, D., Pugachov, D., Rehlich, K., Richter, D., Riemann, S., Ross, M., Rossbach, J., Sachwitz, M., E.L.Saldin, Sandner, W., Schlarb, H., Schmidt, B., Schmitz, M., Schümser, P., Schneider, J., Schneidmiller, E., Schreiber, H.-J., Schreiber, S., Shabunov, A., Sertore, D., Setzer, S., Simrock, S., Sombrowski, E., Staykov, L., Steffen, B., Stephan, F., Stulle, F., Sytchev, K., Thom, H., Tiedtke, K., Tischer, M., Treusch, R., Trines, D., Tsakov, I., Vardanyan, A., Wanzenberg, R., Weiland, T., Weise, H., Wendt, M., Will, I., Winter, A., Wittenburg, K., Yurkov, M., Zagorodnov, I., Zambolin, P., Zapfe, K., 2006. First operation of a free-electron laser generating gw power radiation at 32 nm wavelength. Eur. J. Phys. D. 37, 297–303.

Ayvazyan, V., Baboi, N., Bohnet, I., Bolzmann, A., Brinkmann, R., Castro, P., Catani, L., Choroba, S., Cianchi, A., Dohlus, M., Edwards, H., Faatz, B., Fateev, A., Feldhaus, J., Flöttmann, K., Gamp, A., Garvey, T., Genz, H., Gerth, C., Gretchko, V., Grigoryan, B., Hahn, U., Hessler, C., Honkavaara,

K., Hüning, M., Ischebeck, R., Jablonka, M., Kamps, T., Körfer, M., Krassilnikov, M., Krzywinski, J., Liepe, M., Liero, A., Limberg, T., Loos, H., Luong, M., Magne, C., Menzel, J., Michelato, P., Minty, M., Müller, W., Nölle, D., Novokhatski, A., Pagani, C., Peters, F., Pflüger, J., Piot, P., Plucinski, L., Rehlich, K., Reyzl, I., Richter, A., Rossbach, J., E.L.Saldin, Sandner, W., Schlarb, H., Schmidt, B., Schmitz, M., Schümser, P., Schneider, J., Schneidmiller, E., Schreiber, H.-J., Schreiber, S., Sertore, D., Setzer, S., Simrock, S., Sobierajski, R., Sonntag, B., Steed, B., F. Stephan, K. S., Tiedtke, K., Tonutti, M., Treusch, R., Trines, D., Türke, D., Verzilov, V., Wanzenberg, R., Weiland, T., Weise, H., Wendt, M., Will, I., Wolff, S., Wittenburg, K., Yurkov, M., Zapfe, K., 2002a. Generation of gw radiation pulses from a vuv free-electron laser operating in the femtosecond regime. Phys. Rev. Lett. 88, 104802.

Ayvazyan, V., Baboi, N., Bohnet, I., Brinkmann, R., Castellano, M., Castro, P., Catani, L., Choroba, S., Cianchi, A., Dohlus, M., Edwards, H. T., Faatz, B., Fateev, A. A., Feldhaus, J., Flöttmann, K., Gamp, A., Garvey, T., Genz, H., Gerth, C., Gretchko, V., Grigoryan, B., Hahn, U., Hessler, C., Honkavaara, K., Hüning, M., Ischebeck, R., Jablonka, M., Kamps, T., Körfer, M., Krassilnikov, M., Krzywinski, J., Liepe, M., Liero, A., Limberg, T., Loos, H., Luong, M., Magne, C., Menzel, J., Michelato, P., Minty, M., Müller, U.-C., Nölle, D., Novokhatski, A., Pagani, C., Peters, F., Pflüger, J., Piot, P., Plucinski, L., Rehlich, K., Reyzl, I., Richter, A., Rossbach, J., Saldin, E. L., Sandner, W., Schlarb, H., Schmidt, G., Schmüser, P., Schneider, J. R., Schneidmiller, E. A., Schreiber, H.-J., Schreiber, S., Sertore, D., Setzer, S., Simrock, S., Sobierajski, R., Sonntag, B., Steeg, B., Stephan, F., Sytchev, K. P., Tiedtke, K., Tonutti, M., Treusch, R., Trines, D., Türke, D., Verzilov, V., Wanzenberg, R., Weiland, T., Weise, H., Wendt, M., Wilhein, T., Will, I., Wittenburg, K., Wolff, S., Yurkov, M. V., Zapfe, K., 2002b. A new powerful source for coherent vuv radiation: Demonstration of exponential growth and saturation at the ttf free-electron laser. Eur. J. Phys. D. 20, 149–156.

Bartell, L. S., Huang, J., 1994. Supercooling of water below the anomalous range near 226 k. J. Phys. Chem. 98, 7455–7457.

Bentson, L., Emma, P., Krejcik, P., 2002. A new bunch compressor chicane for the slac linac to produce 30-fsec, 30-ka, 30-gev electron bunches. In: Garvey, T., Duff, J. L., Roux, P. L., Petit-Jean-Genaz, C., Poole, J., Rivkin, L. (Eds.), Proceedings of European Particle Accelerator Conference, 2002, Paris, France. CERN, Geneve, pp. 683–685.

Berendsen, H. J. C., Postma, J. P. M., van Gunsteren, W. F., Hermans, J., 1981. Interaction models for water in relation to protein hydration. In: Pullman, B. (Ed.), Intermolecular Forces. D. Reidel Publishing Company, Dordrecht, pp. 331–342.

Berendsen, H. J. C., van der Spoel, D., van Drunen, R., 1995. GROMACS: A message-passing parallel molecular dynamics implementation. Comp. Phys. Comm. 91, 43–56.

Bergh, M., Tîmneanu, N., van der Spoel, D., 2004. A model for the dynamics of a water cluster in a X-ray FEL beam. Phys. Rev. **E** 70, 051904.

Bernal, J. D., Fankuchen, I., Perutz, M. F., 1938. An x-ray study of chymotrypsin and haemoglobin. Nature 141, 523–524.

Bethe, H., 1930. Zur theorie des durchgangs schneller korpuskularstrahlen durch materie. Ann. Phys. 5, 325–400.

Bragg, L., Perutz, F. M., 1952. The structure of haemoglobin. Proc. R. Soc. London Ser. A 213, 425–435.

Brook, E., Harrison, M. F. A., Smith, A. C. H., 1978. Measurements of the electron impact ionisation cross sections of he, c, 0 and n atoms. btjphb 11, 3115–3132.

Bukowski, R., Szalewicz, K., Groenenboom, G. C., van der Avoird, A., 2007. Predictions of the properties of water from first principles. Science 315, 1249–1252.

Carlson, L.-A., 2006. On the feasibility of nuclear fusion experiments with xuv and x-ray free-electron lasers (UPTEC X 06 024). Master's thesis, Uppsala University.

Cavalieri, A. L., Fritz, D. M., Lee, S. H., Bucksbaum, P. H., Reis, D. A., Rudati, J., Mills, D. M., Fuoss, P. H., Stephenson, G. B., Kao, C. C., Siddons, D. P., Lowney, D. P., MacPhee, A. G., Weinstein, D., Falcone, R. W., Pahl, R., Als-Nielsen, J., Blome, C., Düsterer, S., Ischebeck, R., Schlarb, H., Schulte-Schrepping, H., Tschentscher, T., Schneider, J., Hignette, O., Sette, F., Sokolowski-Tinten, K., Chapman, H. N., Lee, R. W., Hansen, T. N., Synnergren, O., Larsson, J., Techert, S., Sheppard, J., Wark, J. S., Bergh, M., Caleman, C., Huldt, G., van der Spoel, D., Timneanu, N., Hajdu, J., Akre, R. A., Bong, E., Emma, P., Krejcik, P., Arthur, J., Brennan, S., Gaffney, K. J., Lindenberg, A. M., Luening, K., Hastings, J. B., 2005. Clocking femtosecond x rays. Phys. Rev. Lett. 94, 114801.

Creuzburg, M., 1966. Energieverlustspektren der alkalihalogenide und der metalle cu, ag und au und vergleich mit optischen messungen. Z. Phys. 196, 433–463.

Darden, T., York, D., Pedersen, L., 1993. Particle mesh Ewald: An N-log(N) method for Ewald sums in large systems. J. Chem. Phys. 98, 10089–10092.

Dobson, C. M., 2004. Chemical space and biology. Nature 432, 824–828.

Dole, M., Mach, L. L., Hines, R. L., Ferguson, L. P., Alice, M. B., 1968. Molecular beams of macroions. J. Chem. Phys. 49, 2240–2249.

Drude, P. K. L., 1900. Zur elektronentheorie der metalle. Annalen der Physik 306, 566–613.

Düsterer, S., Radcliffe, P., Geloni, G., Jastrow, U., Kuhlmann, M., Plönjes, E., Tiedtke, K., Treusch, R., a nd P. Nicolosi, J. F., Poletto, L., Yeates, P., Luna, H., Costello, J. T., Orr, P., Cubaynes, D., Meyer, M., 2006. Spectroscopic characterization of vacuum ultraviolet free electron laser pulses. Opt. Lett. 31, 1750–1752.

Emma, P., 2002. Accelerator physics challenges of x-ray fel sase sources. In: Garvey, T., Duff, J. L., Roux, P. L., Petit-Jean-Genaz, C., Poole, J., Rivkin, L. (Eds.), Proceedings of European Particle Accelerator Conference, 2002, Paris, France. CERN, Geneve, pp. 49–53.

Ewald, P. P., 1921. Die Berechnung optischer und elektrostatischer Gitterpotentiale. Ann. Phys. 64, 253–287.

Fermi, E., 1924. Z. Phys. 29, 315.

Frank, J., 1996. Three-Dimensional Electron Microscopy of Macromolecular Assemblies. Academic Press, San Diego.

Fritz, D. M., Reis, D. A., Adams, B., Akre, R. A., Arthur, J., Blome, C., Bucksbaum, P. H., Cavalieri, A. L., Engemann, S., Fahy, S., Falcone, R. W., Fuoss, P. H., Gaffney, K. J., George, M. J., Hajdu, J., Hertlein, M. P., Hillyard, P. B., von Hoegen, M. H., Kammler, M., Kaspar, J., Kienberger, R., Krejcik, P., Lee, S. H., Lindenberg, A. M., McFarland, B., Meyer, D., Montagne, T., Murray, E. D., Nelson, A. J., Nicoul, M., Pahl, R., Rudati, J., Schlarb, H., Siddons, D. P., Sokolowski-Tinten, K., Tschentscher, T., von der Linde, D., Hastings, J. B., 2007. Ultrafast bond softening in bismuth: Mapping a solid's interatomic potential with x-rays. Science 315, 633–636.

Gerchberg, R. W., Saxton, W. O., 1972. A practical algorithm for the determination of phase from image and diffraction plane pictures. Optik 35, 237–246.

Guillot, B., 2002. A reappraisal of what we have learnt during three decades of computer simulations on water. J. Mol. Liq. 101, 219–260.

Hajdu, J., 1990. Laue crystallography of macromolecules. In: Jensen, B., Jørgensen, F. S., Kofod, H. (Eds.), Frontiers in drug research, Alfred Benzon Symposium 28. Munksgaard, Copenhagen, pp. 375–395.

Hajdu, J., 1994. Towards femtosecond time resolution in broad-band laue diffraction studies - a possibility. In: Arthur, J., Materlik, G., Winnick, H. (Eds.), Scientific Applications of Coherent X-rays. SLAC/SSRL-0066, SLAC, pp. 91–94.

Hajdu, J., 2000. Single-molecule x-ray diffraction. Curr. Op. Struct. Biol. 10, 569–573.

Hajdu, J., Hodgson, K., Miao, J., van der Spoel, D., Neutze, R., Robinson, C. V., Faigel, G., Jacobsen, C., Kirz, J., Sayre, D., Weckert, E., Materlik, G., Szőke, A., 2000. Structural studies on single particles and biomolecules. In: LCLS: The First Experiments. SSRL, SLAC, Stanford, USA, pp. 35–62.

Hau-Riege, S. P., London, R. A., Huldt, G., Chapman, H. N., 2005. Pulse requirements for x-ray diffraction imaging of single biological molecules. Phys. Rev. **E** 71, 061919.

Hau-Riege, S. P., London, R. A., Szőke, A., 2004. Dynamics of biological molecules irradiated by short x-ray pulses. Phys. Rev. **E** 69, 051906.

Hau-Riege, S. P., London, R. A., Szőke, A., 2004. Dynamics of biological molecules irradiated by short x-ray pulses. Phys. Rev. **E** 69, 051906.

Hayward, S., Kitao, A., Berendsen, H. J. C., 1997. Model-free method of analyzing domain motions in proteins from simulation: a comparison of normal mode analysis and molecular dynamics methods. PROTEINS: Struct. Funct. Gen. 27, 425–437.

Hedin, L., 1965. New method for calculating the one-particle green's function with application to the electron-gas problem. Phys. Rev. 139, A796–A823.

Henderson, R., 1995. The potential and limitations of neutrons, electrons and X-rays for atomic resolution microscopy of unstained biological molecules. Quart. Rev. Biophys. 28, 171–193.

Henke, B. L., 1972. Ultrasoft-x-ray reflection, refraction, and production of photoelectrons (100-1000-ev region). Phys. Rev. **A** 6, 94–104.

Henke, B. L., Liesegang, J., Smith, S. D., 1979. Soft-x-ray-induced secondary-electron emission from semiconductors and insulators: Models and measurements. Phys. Rev. **B** 19, 3004–3021.

Hentschel, M., Kienberger, R., Spielmann, C., Reider, G. A., Milosevic, N., Brabec, T., Corkum, P., Heinzmann, U., Drescher, M., Krausz, F., 2001. Attosecond metrology. Nature 414, 509–513.

Hockney, R. W., Eastwood, J. W., 1981. Computer simulation using particles. McGraw-Hill, New York.

Huang, J., Bartell, L. S., 1995. Kinetics if homogeneous nucleation in the freezing of large water clusters. J. Phys. Chem. 99, 3924–3931.

Hubbell, J. H., Veigele, W. J., Briggs, E. A., Brown, R. T., Cromer, D. T., Howerton, R. J., 1975. Atomic form factors, incoherent scattering functions, and photon scattering cross sections. J. Phys. Chem. Ref. Data 4, 471–494.

Huldt, G., Szőke, A., Hajdu, J., 2003. Diffraction imaging of single particles and biomolecules. J. Struct. Biol. 144, 219–227.

Iavarone, A., Parks, J., 2005. Conformational change in unsolvated trp-cage protein probed by fluorescence. J. Am. Chem. Soc. 127, 8606–8607.

Iglev, H., Schmeisser, M., Simeonidis, K., Thaller, A., Laubereau, A., 2006. Ultrafast superheating and melting of bulk ice. Nature 439, 183–186.

Jarrold, M. F., 1999. Unfolding, refolding and hydration of protein ions in the gas phase. Acc. Chem. Res. 32, 360–367.

Jorgensen, W. L., Chandrasekhar, J., Madura, J. D., Impey, R. W., Klein, M. L., 1983. Comparison of simple potential functions for simulating liquid water. J. Chem. Phys. 79, 926–935.

Jurek, Z., Faigel, G., Tegze, M., 2004a. Dynamics in a cluster under the influence of intense femtosecond hard X-ray pulses. Eur. Phys. J. D 29, 217–229.

Jurek, Z., Oszlányi, G., Faigel, G., 2004b. Imaging atom clusters by hard x-ray free-electron lasers. Europhys. Lett. 65, 491–497.

Kaku, M., 1993. Quantum Field Theory. Oxford University Press, New York.

Kane, E. O., 1966. Simple model for collision effects in photoemission. Phys. Rev. 147, 335.

Kebarle, P., Tang, L., 1993. From ions in solution to ions in the gas-phase - the mechanism of electrospray mass-spectrometry. Anal. Chem. 65, 972A–986A.

Key, M. H., Lewis, C. L. S., Lunney, J. G., Moore, A., Ward, M., Thareja, R. K., 1980. Time-resolved x-ray spectroscopy of laser-produced plasmas. Phys. Rev. Lett. 44, 1669–1672.

Kim, Y.-K., Rudd, M. E., 1994. Binary-encounter-dipole model for electron-impact ionization. Phys. Rev. **A** 50, 3954.

Kittel, C., 1996. Introduction to Solid State Physics. John Wiley & Sons Inc., New York.

Kohn, W., Sham, L. J., 1965. Self-consistent equations including exchange and correlation effects. Phys. Rev. 140, a1133.

Krause, M. O., Oliver, J. H., 1979. Natural width of atomic K and L level Kα X-ray lines and several KLL Auger lines. J. Phys. Chem. Ref. Data 8, 329–338.

Kushwaha, M. S., 1981. Compressibilities, debye-waller factors, and melting criteria for ii-vi and iii-v compound semiconductors. Phys. Rev. **B** 24, 2115–2120.

Landau, L. D., Lifschitz, E. M., 1977. Quantum Mechanics (Non-relativistic Theory), 3rd Edition. Pergamon Press, Oxford.

Lawrence, C. P., Skinner, J. L., 2003. Flexible tip4p model for molecular dynamics simulation of liquid water. Chem. Phys. Lett. 372, 842–847.

Leach, A. R., 2001. Molecular modelling: principles and applications. Prentice Hall, New York.

Lennon, M. A., Bell, K. L., Gilbody, H. B., Hughes, J. G., Kingston, A. E., Murray, M. J., Smith, F. J., 1988. Recommended data on electron impact ionization of atoms and ions: Fluorine to nickel. J. Phys. Chem. Ref. Data 17, 1285–1363.

Lindahl, E., Hess, B. A., van der Spoel, D., 2001. GROMACS 3.0: A package for molecular simulation and trajectory analysis. J. Mol. Mod. 7, 306–317.

Lindemann, F. A., 1919. über die berechnung molekularer eigenfrequenzen. Z. Phys. 11, 609.

Lindhard, J., 1954. K. Dan. Vidensk. Selsk. Mat. Fys. Medd. 28, 1.

Lowney, D. P., Heimann, P. A., Padmore, H. A., Gullikson, E. M., MacPhee, A. G., Falcone, R. W., 2004. Characterization of csi photocathodes at grazing incidence for use in a unit quantum efficiency x-ray streak camera. Rev. Sci. Instrum. 75, 3131–3137.

Mahoney, M. W., Jorgensen, W. L., 2000. A five-site model for liquid water and the reproduction of the density anomaly by rigid, nonpolarizable potential functions. J. Chem. Phys. 112, 8910–8922.

Marchesini, S., Chapman, H. N., Hau-Riege, S. P., London, R. A., Szőke, A., 2003a. Coherent x-ray diffractive imaging: applications and limitations. Opt. Express 11, 2344–2353.

Marchesini, S., He, H., Chapman, H. N., Hau-Riege, S. P., Noy, A., Howells, M. R., Weierstall, U., Spence, J. C. H., 2003b. X-ray image reconstruction from a diffraction pattern alone. Phys. Rev. **B** 114, 140101.

Marcus, Y., 1994. A simple empirical model describing the thermodynamics of hydration of ions of widely varying charges, sizes, and shapes. Bioph. Chem. 51, 111–127.

Marginean, I., Znamenskiy†, V., Vertes, A., 2006. Charge reduction in electrosprays: Slender nanojets as intermediates. J. Phys. Chem. B. 110, 6397–6404.

Massimi, M., 2005. Pauli's Exclusion Principle. Cambridge University Press, Cambridge, United Kingdom.

Matsumoto, M., Saito, S., Ohmine, I., 2002. Molecular dynamics simulation of the ice nucleation and growth process leading to water freezing. Nature 416, 409–413.

Miao, J., Hodgson, K., Sayre, D., 2001. An approach to three-dimensional structures of biomolecules by using single-molecule diffraction images. Proc. Natl. Acad. Sci. U.S.A. 98, 6641–6645.

Miao, J., Hodgson, K. O., Ishikawa, T., Larabell, C. A., LeGros, M. A., Nishino, Y., 2003. Imaging whole escherichia coli bacteria by using single particle x-ray diffraction. Proc. Natl. Acad. Sci. U.S.A. 100, 110–112.

Miao, J., Ishikawa, T., Johnson, B., Anderson, E. H., Lai, B., Hodgson, K. O., 2006. High resolution 3d x-ray diffraction microscopy. Phys. Rev. Lett. 89, 088303.

Morse, P. M., 1929. Diatomic molecules according to the wave mechanics. II. vibrational levels. Phys. Rev. 34, 57–64.

Muroya, Y., Meesungnoen, J., Jay-Gerin, J.-P., Filali-Mouhim, A., Goulet, T., Katsumura, Y., Mankhetkorn, S., 2002. Radiolysis of liquid water: An attempt to reconcile monte-carlo calculations with new experimental hydrated electron yield data at early times. Can. J. Chem. 80, 1367–1374.

Neutze, R., Hajdu, J., 1997. Femtosecond time resolution in X-ray diffraction experiments. Proc. Natl. Acad. Sci. U.S.A. 94, 5651–5655.

Neutze, R., Huldt, G., Hajdu, J., van der Spoel, D., 2004. Potential impact of an X-ray free electron laser on structural biology. Radiat. Phys. Chem. 71, 905–916.

Neutze, R., Wouts, R., van der Spoel, D., Weckert, E., Hajdu, J., 2000. Potential for biomolecular imaging with femtosecond X-ray pulses. Nature 406, 752–757.

Newton, I., 1687. Philosophiae naturalis principia mathematica. London.

Patriksson, A., Adams, C., Kjeldsen, F., Raber, J., van der Spoel, D., Zubarev, R. A., 2006. Prediction of N-C_O bond cleavage frequencies in electron capture dissociation of Trp-cage dications by force-field molecular dynamics simulations. Int. J. Mass Spectrom. 248, 124–135.

Patriksson, A., Marklund, E., van der Spoel, D., 2007. Protein structures under electrospray conditions. Biochemistry 46, 933–945.

Penn, D. R., 1976. Electron mean free paths for free-electron-like materials. Phys. Rev. **B** 13, 674.

Penn, D. R., 1987. Electron mean-free-path calculations using a model dielectric function. Phys. Rev. **B** 35, 483.

Perez, D., Lewis, L. J., 2003. Molecular-dynamics study of ablation of solids under femtosecond laser pulses. Phys. Rev. **B** 67, 184102.

Persson, P., Lunell, S., Szőke, A., Ziaja, B., Hajdu, J., 2001. Shake-up and shake-off excitations with associated electron losses in x-ray studies of proteins. Prot. Sci. 10, 2480–2484.

Rayleigh, L., 1882. On the equilibrium of liquid conducting masses charged with electricity. Phil. Mag. 14, 184–186.

Robinson, I. K., Vartanyants, I. A., Williams, G. J., Pfeifer, M. A., Pitney, J. A., 2001. Reconstruction of the shapes of gold nanocrystals using coherent x-ray diffraction. Phys. Rev. Lett. 87, 195505.

Sayre, D., 1952. Some implications of a theorem due to shannon. Anal. Chem. 5, 843.

Sayre, D., 2002. X-ray crystallography. Struct. Chem. 13, 81–96.

Shannon, C. E., 1949. Communications in the presence of noise. Proceedings of the Institute of Radio Engineers 37, 10–21.

Siegbahn, K., Nordling, C., Johansson, G., Hedman, J., Heden, P. H., Hamrin, K., Gelius, U., Bergmark, T., Werme, L. O., Manne, R., Bear, Y., 1969. ESCA applied to free molecules. North Holland, Amsterdam.

Silkin, V. M., Chulkov, E. V., Echenique, P. M., 2003. First-principles calculation of the electron inelastic mean free path in be metal. Phys. Rev. **B** 68, 205106.

Solem, J. C., 1986. Imaging biological specimens with high-intensity soft X-rays. J. Opt. Soc. Am. B. 3, 1551–1565.

Stein, G. D., Armstrong, J. A., 1973. Structure of water and carbon dioxide clusters formed via homogeneous nucleation in nozzle beams. J. Chem. Phys. 58, 1999–2003.

Svishchev, I. M., Kusalik, P. G., 1994. Crystallisation of liquid water in a molecular dynamics simulation. Phys. Rev. Lett. 73, 975–978.

Synnergren, O., 2005. Time-resolved x-ray diffraction studies of phonons and phase transitions. Ph.D. thesis, Malmö Universitet, Malmö Sweden.

Synnergren, O., Harbst, M., Missalla, T., Larsson, J., Katona, G., Neutze, R., Wouts, R., 2002. Projecting picosecond lattice dynamics through x-ray topography. Appl. Phys. Lett. 80, 3727–3729.

Tang, L., Kebarle, P., 1993. Dependence of ion intensity in electrospray mass spectrometry on the concentration of the analytes in the electrosprayed solution. Anal. Chem. 65, 3654–3668.

Tanuma, S., Powell, C. J., Penn, D. R., 1988. Calculations of electron inelastic mean free paths for 31 materials. Surf. Interface Anal. 11, 577–589.

Tanuma, S., Powell, C. J., Penn, D. R., 1991a. Calculations of electron inelastic mean free paths ii. data for 27 elements over the 50-2000 ev range. Surf. Interface Anal. 17, 911–926.

Tanuma, S., Powell, C. J., Penn, D. R., 1991b. Calculations of electron inelastic mean free paths iii. data for 15 inorganic compounds over the 50-2000 ev range. Surf. Interface Anal. 17, 927–939.

Tanuma, S., Powell, C. J., Penn, D. R., 1993a. Calculations of electron inelastic mean free paths (imfps) iv. evaluation of the calculated imfps and of the predictive imfp formula tpp-2 for electron energies between 50 and 2000 ev. Surf. Interface Anal. 20, 77–89.

Tanuma, S., Powell, C. J., Penn, D. R., 1993b. Calculations of electron inelastic mean free paths v. data for 14 organic compounds over the 50-2000 ev range. Surf. Interface Anal. 21, 165–176.

Thompson, A. C., Vaughan, D. (Eds.), 2001. X-ray Data Booklet, 2nd Edition. Lawrence Berkeley National Laboratory, Berkeley.

Tito, M. A., Tars, K., Valegård, K., Hajdu, J., Robinson, C. V., 2000. Electrospray time-of-flight mass spectrometry of the intact ms2 virus capsid. J. Am. Chem. Soc. 122, 3550–3551.

van der Spoel, D., Lindahl, E., Hess, B., Groenhof, G., Mark, A. E., Berendsen, H. J. C., 2005. GROMACS: Fast, Flexible and Free. J. Comp. Chem. 26, 1701–1718.

van der Spoel, D., van Maaren, P. J., 2006. The origin of layer structure artifacts in simulations of liquid water. J. Chem. Theor. Comp. 2, 1–11.

van Heel, M., Gowen, B., Matadeen, R., Orlova, E. V., Finn, R., Pape, T., Cohen, D., Stark, H., Schmidt, R., Schatz, M., Patwardhan, A., 2000. Single-particle electron cryo-microscopy: towards atomic resolution. Quart. Rev. Biophys. 33, 307–269.

Veigele, W. J., 1973. Photon cross sections from 0.1 keV to 1 MeV for elements with Z=1 to Z=94. Atomic Data 5, 51–111.

Velazquez, I., Reimann, C. T., Tapia, O., 1999. Proteins in vacuo: Relaxation of unfolded lysozyme leads to folding into native and non-native structures. A molecular dynamics study. J. Am. Chem. Soc. 121, 11468–11477.

Verma, R. L., 1973. Secondary electron emission of caesium iodide. J. Phys. D: Appl. Phys. 6, 2137–2141.

Vurgaftmana, I., Meyer, J. R., Ram-Mohan, L. R., 2001. Band parameters for iii – v compound semiconductors and their alloys. J. Appl. Spectrosc. 89, 5815–5875.

Wagner, C. D., Zatko, D. A., Raymond, R. H., 1980. Use of the oxygen KLL Auger lines in identification of surface chemical states by electron spectroscopy for chemical analysis. Anal. Chem. 52, 1445–1451.

Warren, B. E., 1990. X-ray Diffraction. Dover Publications Inc., New York.

Weast, R. C., 1977. Handbook of Chemistry and Physics. CRC Press, Cleveland, Ohio.

Yamashita, M., Fenn, J. B., 1984a. Electrospray ion source. another variation on the free-jet theme. J. Phys. Chem. 88, 4451–4459.

Yamashita, M., Fenn, J. B., 1984b. Negative ion production with the electrospray ion source. J. Phys. Chem. 88, 4671–4675.

Zakharov, V. V., Brodskaya, E. N., Laaksonen, A., 1998. Surface properties of water clusters: a molecular dynamics study. Mol. Phys. 95, 203–209.

Zangi, R., Mark, A. E., 2003. Monolayer ice. Phys. Rev. Lett. 91, 025502.

Ziaja, B., de Castro, A., Weckert, E., Möller, T., 2006. Modelling dynamics of samples exposed to free-electron-laser radiation with boltzmann equations. Eur. J. Phys. D. 40, 465–480.

Ziaja, B., London, R. A., Hajdu, J., 2005. Unified model of secondary electron cascades in diamond. J. Appl. Phys. 97, 064905.

Ziaja, B., Szőke, A., van der Spoel, D., Hajdu, J., 2002. Space-time evolution of electron cascades in diamond. Phys. Rev. **B** 66, 024116.

Ziaja, B., van der Spoel, D., Szőke, A., Hajdu, J., 2001. Radiation induced electron cascade in diamond and amorphous carbon. Phys. Rev. **B** 64, 214104.

Acta Universitatis Upsaliensis

Digital Comprehensive Summaries of Uppsala Dissertations from the Faculty of Science and Technology 315

Editor: The Dean of the Faculty of Science and Technology

A doctoral dissertation from the Faculty of Science and Technology, Uppsala University, is usually a summary of a number of papers. A few copies of the complete dissertation are kept at major Swedish research libraries, while the summary alone is distributed internationally through the series Digital Comprehensive Summaries of Uppsala Dissertations from the Faculty of Science and Technology. (Prior to January, 2005, the series was published under the title "Comprehensive Summaries of Uppsala Dissertations from the Faculty of Science and Technology".)

Distribution: publications.uu.se
urn:nbn:se:uu:diva-7915

ACTA
UNIVERSITATIS
UPSALIENSIS
UPPSALA
2007